

Synthesis of PVC-co-PVAc-co-PVA/Cu Nanocomposites with Improved Dielectric Performance



Mehwish Younas
NUST201463659MSNS78214F

A thesis submitted in partial fulfillment of requirements for the degree of

Master of Science in Chemistry

Supervised by: **Prof. Ilyas Sarwar**

Co-supervised by: **Dr. Mudassir Iqbal**

Department of Chemistry

National University of Sciences and Technology

Islamabad, Pakistan

2017

National University of Sciences & Technology**MS THESIS WORK**

We hereby recommend that the dissertation prepared under our supervision by: MEHWISH YOUNAS, Regn No. NUST201463659MSNS78214F Titled: Synthesis of PVC-co-PVAc-co-PVA/Cu nanocomposites with improved dielectric performance be accepted in partial fulfillment of the requirements for the award of **MS** degree.

Examination Committee Members

1. Name: PROF. NASIR MAHMOOD AHMED Signature: 

2. Name: DR. AZHAR MAHMOOD Signature: 

External Examiner: DR. SAIMA KALSOOM Signature: 

Co-Supervisor's Name: DR. MUDASSIR IQBAL Signature: 

Supervisor's Name: PROF. M. ILYAS SARWAR Signature: 


Head of Department

15-11-17
Date


COUNTERSIGNED


Date: 15/11/17



Dean/Principal

THESIS ACCEPTANCE CERTIFICATE

Certified that final copy of MS thesis written by Ms. Mehwish Younas, (Registration No. NUST201463659MSNS78214F), of School of Natural Sciences has been vetted by undersigned, found complete in all respects as per NUST statutes/regulations, is free of plagiarism, errors, and mistakes and is accepted as partial fulfillment for award of MS/M.Phil degree. It is further certified that necessary amendments as pointed out by GEC members and external examiner of the scholar have also been incorporated in the said thesis.

Signature: 
Name of Supervisor: Prof. M. Ilyas Sarwar
Date: 15.11.2017

Signature (HoD): 
Date: 15-11-17

Signature (Dean/Principal): 
Date: 15/11/17

*In the Name of Allah, the most
Compassionate and the most
Merciful*

*Dedicated to,
My parents and siblings*

Table of Contents

List of Abbreviations.....	vii
List of Figures	xi
List of Tables.....	xii
Acknowledgments.....	xiv
Abstract	xv
Chapter 1 Introduction	16
1.1. Nanoscience and Nanocomposites:	16
1.2. Classification of Nanocomposites:	16
1.2.1. Ceramic Matrix Nanocomposite:	17
1.2.2. Metal Matrix Nanocomposite:	17
1.2.3. Polymer Matrix Nanocomposite:	17
1.3. Properties of Polymeric Nanocomposite:	18
1.3.1. Dielectric Properties:.....	18
1.3.2. Mechanical Properties:.....	19
1.3.3. Thermal Properties:.....	19
1.4. Applications of Polymeric Nanocomposites:	19
1.4.1. Electronics.....	20
1.4.2. Aerospace.....	20
1.4.3. Biomedical	21
1.4.4. Packaging	21
1.5. Characterization Techniques	22
1.5.1 X-ray Diffraction.....	22
1.5.1.1 Fundamental Principle.....	22
1.5.1.2 Instrumentation of X-ray Powder Diffraction.....	23

1.5.2	Scanning Electron Microscopy	24
1.5.2.1	Working of SEM.....	25
1.5.2.2	Fundamental Principles of Scanning Electron.....	25
1.5.2.3	Instrumentation of SEM.....	26
1.5.3	Infrared Spectroscopy	29
1.5.3.1	Principle.....	29
1.5.3.2	Instrumentation.....	30
1.5.4	LCR Meter.....	32
1.5.4.1	Fundamental Principle and Working of LCR Meter.....	33
Chapter 2 Literature Survey		35
2.1.	Copper Nanoparticles	35
2.1.1.	Synthesis of Copper Nanoparticles:	35
2.1.2.	Application of Copper Nanoparticles.....	36
2.1.3.	Synthesis and Properties of Copper based Polymeric Nanocomposite.....	37
2.1.4.	Synthesis of Poly (vinyl chloride-co-vinyl acetate-co- vinyl alcohol) based Nanocomposites	40
Chapter 3 Experimentation.....		41
3.1	Experimental Work.....	41
3.1.1	Polyol method for Copper Nanoparticle Synthesis	41
3.1.2	Synthesis of Copper Nanoparticles	42
3.1.3	Mechanism of Reaction.....	43
3.1.4	Synthesis of PNCs Thin Films	44
Chapter 4 Results and Discussion		47
4.1	X-Ray Powder Diffraction (XPRD)	47
4.2	Field Emission Scanning Electron Microscopy (FESEM).....	49
4.3	Fourier Transform Infrared Spectroscopy (FTIR).....	53

4.4 Properties	55
4.4.1 Dielectric Properties:.....	55
4.5 Conclusion and Future Prospects:	60
References	62

List of Abbreviations

A	Ampere
AA	Ascorbic Acid
Ag	Silver
Al ₂ O ₃	Aluminium Oxide
BSE	Back Scattered Electron
C	Coulomb
C/C	Carbon Reinforced Carbon
CNT	Carbon Nanotubes
CMNCs	Ceramic Matrix Nanocomposites
Co	Cobalt
Cr	Chromium
CTAB	Cetyl Trimethylammonium Bromide
Cu	Copper
CuCl ₂	Copper Chloride
Cu(NO ₃) ₂ .3H ₂ O	Copper Nitrate Trihydrate
Cu(acetate) ₂ .H ₂ O	Copper Acetate Monohydrate
Cu(acac) ₂	Copper Acetylacetonate
CuSO ₄ .5H ₂ O	Copper Sulphate Pentahydrate
DI	Deionized

DEG	Diethylene Glycol
DMAc	Dimethylacetamide
DUT	Device under Test
EDX	Energy Dispersive X-ray Spectroscopy
E. coli	<i>Escherichia coli</i>
EG	Ethylene Glycol
Fe	Iron
F	Farad
IR	Infrared
Kg	Kilogram
KOH	Potassium Hydroxide
kV	Kilo Volt
LCR	Inductance, Capacitance and Resistance
LCD	Liquid Crystal Display
LED	Light Emitting Diode
MMNCs	Metal Matrix Nanocomposites
Mg	Magnesium
MgO	Magnesium Oxide
min	Minutes
NaH ₂ PO ₂ ·2H ₂ O	Sodium Phosphinate Monohydrate
NaBH ₄	Sodium Borohydride
Ni	Nickel

nm	Nanometer
Nm ⁻²	Newton per Meter Square
N ₂ H ₄	Hydrazine
N ₂	Nitrogen
ODA	Oxydianiline
PMNCs	Polymer Matrix Nanocomposites
PAN	Polyacrylonitrile
PANI	Polyaniline
PGMA	Poly (Glycidyl methacrylate)
PMDA	Pyromellitic Dianhydride
PVA	Polyvinyl Alcohol
PVAc	Polyvinyl Acetate
PVC	Polyvinyl Chloride
PVDF	Polyvinylidene Fluoride
PVP	Polyvinyl Pyrrolidone
SED	Secondary Electron Detector
SEM	Scanning Electron Microscopy
sec	Second
SiC	Silicon Carbide
SiO ₂	Silicon dioxide
<i>S. aureus</i>	<i>Staphylococcus aureus</i>
TiO ₂	Titania

THF	Tetrahydrofuran
V	Volt
Wt	Weight
XPRD	X-ray Powder Diffraction
ZnO	Zinc oxide
°C	degree Celsius
$\ln(F)$	Natural log of Frequency
ε	Dielectric Constant
ε''	Dielectric loss
σ_{ac}	AC Conductivity
$\tan\delta$	Tangent loss
%	Percent

List of Figures

<i>Figure 1.1: Types of nanocomposites</i>	17
<i>Figure 1.2: Applications of polymeric nanocomposites</i>	20
<i>Figure 1.3: X-ray diffraction</i>	23
<i>Figure 1.4: X-ray diffractometer</i>	24
<i>Figure 1.5: Schematic diagram of SEM</i>	26
<i>Figure 1.6: Secondary electron detector</i>	28
<i>Figure 1.7: Electromagnetic radiation spectrum</i>	29
<i>Figure 1.8: Energy level in IR</i>	30
<i>Figure 1.9: Instrumentation of IR spectrometer</i>	32
<i>Figure 1.10: Circuit diagram for Wheatstone bridge method</i>	33
<i>Figure 1.11: Circuit diagram of LCR meter at low voltage</i>	34
<i>Figure 1.12: Circuit diagram of LCR meter at high voltage</i>	34
<i>Figure 3.1: Graphical representation of synthesis of Copper nanoparticles</i>	43
<i>Figure 3.2: Flow sheet for synthesis of films</i>	45
<i>Figure 4.1: XPRD pattern of Copper nanoparticles</i>	48
<i>Figure 4.2: XPRD of PVC-co-PVAc-co-PVA/Copper nanocomposite films of various concentrations</i>	49
<i>Figure 4.3: FESEM images and EDX spectra of Copper nanoparticles</i>	50
<i>Figure 4.4(a-e): SEM micrographs of nanoparticle distribution in polymeric nanocomposite films</i>	51

<i>Figure 4.5(a-e): SEM micrographs showing particle size in polymeric nanocomposite films.....</i>	<i>51</i>
<i>Figure 4.6(a-e): EDX spectra of nanocomposite films of various concentrations.....</i>	<i>52</i>
<i>Figure 4.7: Infrared spectra of Copper nanoparticles.....</i>	<i>53</i>
<i>Figure 4.8: IR spectra of Copper nanocomposite films of various concentrations.....</i>	<i>54</i>
<i>Figure 4.9: Dielectric constant of Copper nanocomposite films of various concentrations.....</i>	<i>57</i>
<i>Figure 4.10: Dielectric loss of Copper nanocomposite films of various concentrations.....</i>	<i>58</i>
<i>Figure 4.11: Tan loss of Copper nanocomposite films of various concentrations.....</i>	<i>59</i>
<i>Figure 4.12: AC conductivity of Copper nanocomposite films of various concentrations.....</i>	<i>60</i>

List of Tables

<i>Table 1.1: Different types of nanocomposites</i>	18
<i>Table 3.1: List of chemicals used in the synthesis</i>	42
<i>Table 3.2: List of chemicals used in the synthesis of thin films</i>	44
<i>Table 3.3: Weight percentages of the PVC- co- PVAc -co- PVA and Copper nanoparticles used in the preparation of thin films</i>	46

Acknowledgments

In the name of Allah; the most gracious and most merciful. I would like to praise Allah Almighty for his blessings during my entire MS degree.

*I would like to thank my supervisor, **Prof Dr. Ilyas Sarwar** for his support, guidance and encouragement. He fully guided me during my entire research work. I am thankful for his critical comments and co-operation. I am cordial thankful to my co-supervisor, **Dr. Mudassir Iqbal** for his help during my thesis writing. He always steered me in right direction whenever I needed it. His motivation accomplished me to complete my MS degree.*

*I pay special thank to HoD Chemistry, **Prof Habib Nasir** for listening our research issues and resolving them to their best. I am extremely thankful to my GEC members; **Dr. Azhar Mehmood** and **Dr. Nasir Mahmood** for their suggestions and constructive criticism. I greatly acknowledge the technical facilities provided by SCME NUST.*

*I am thankful to my father **Malik Muhammad Younas** and other family members. A very precious thank to my friends **Maryam Tahir**, **Nitasha Komal**, **Laraib Laiquat** and other batch mates for their immense help.*

Abstract

This thesis reports the synthesis of an easy, environmentally friendly, and cost effective polyol method for the synthesis of copper nanoparticles and copper/poly (vinyl chloride-co-vinyl acetate-co- vinyl alcohol) nanocomposite films using solution casting technique. Face centered cubic structured nanoparticles, space group Fm-3m (225) with average crystallite size of 33.5 nm were successfully prepared with characteristics diffraction peaks at $2\theta = 43.3, 50.5, 73.2^\circ$ as investigated by XPRD. FTIR also shows characteristics band of Cu-PVP hybrid evident in nanoparticles at 1089 and 629 cm^{-1} which further confirm the synthesis of copper nanoparticles.

Polymeric nanocomposite thin films of 5, 10, 15, 20 and 25 % wt were prepared. Polymer show characteristics broad peak ranging from 10-30°. Spherical nanoparticles were seen to be homogenously dispersed in polymer matrix as investigated by Field emission electron spectroscopy (FESEM). Dispersed nanoparticles in the film possess average size of ~68.67 nm. The improved dielectric constants of nanocomposites was as high as 3.75 at 25 % wt. The insulating effect of PVP, coating the copper nanoparticles along with interfacial polarization results in very low value of dielectric loss ranging from 0.08 to 0.16 with tangent loss values at 0.0025 to 0.0054 and range of value of AC conductivity is 0.4×10^{-6} to 1.2×10^{-5} S/m at weight percentage from 5 to 25 of polymeric nanocomposite film which make these nanocomposites films a promising material for used in charge storage applications.

Chapter 1

Introduction

1.1. Nanoscience and Nanocomposites

American physicist Richard Feynman gave the first concept about the “Nanoscience” [1]. “Nanoscience refers to the study of structures with the size range 1 to 100 nm showing properties different from their bulk counterpart and has large surface area to volume ratio.” Nanocomposite is a multiphase solid material where one of the phases has one, two or three dimensions in nanometer (1-100 nm). The solid phase can be amorphous, semi crystalline, grains or combination [2].

Composite materials should have following characteristics.

- Microscopically it is non-homogenous material and has distinct interface.
- There are big differences in performance of component materials.
- The formed composite materials should have great improvement in performance.
- The volume fractions of component materials are larger than 10 % [3].

1.2. Classification of Nanocomposites

Nanocomposite materials can be classified according to their matrix materials in to three different categories.

- a) Ceramic Matrix Nanocomposites (CMNCs)
- b) Metal Matrix Nanocomposites (MMNCs)
- c) Polymer Matrix Nanocomposites (PMNCs) [4]

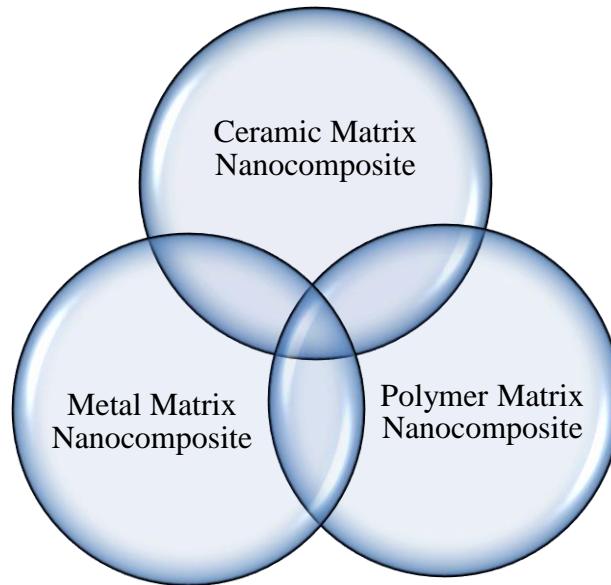


Figure 1.1: Types of nanocomposites.

1.2.1. Ceramic Matrix Nanocomposites

Ceramic Matrix Nanocomposites involve incorporation of ceramics such as chemical compound from group of nitrides, silicides, oxides and borides in ceramic matrix. CMNCs involve the combination of type of fiber/type of matrix e.g. C/C stands for carbon-fiber-reinforced carbon.

1.2.2. Metal Matrix Nanocomposites

Metal Matrix Nanocomposites consist of low density metal such as aluminum or magnesium reinforced with particulate or fibers of ceramic material such as silicon carbide or graphite e.g. carbon fiber used in aluminum matrix.

1.2.3. Polymer Matrix Nanocomposites

Polymeric Matrix Nanocomposites consist of polymer or copolymer having nanoparticles or nanofillers dispersed in matrix e.g. monodispersed copper nanoparticles in polyimide resins [5].

Table 1.1: Different types of nanocomposites.

Types	Examples
Ceramic	Al ₂ O ₃ /SiO ₂ , Al ₂ O ₃ /SiC, Al ₂ O ₃ /TiO ₂ , SiO ₂ /Ni
Metal	Mg/CNT, Fe-Cr/Al ₂ O ₃ , Fe/MgO, Co/Cr
Polymer	Thermoplastic/thermoset, Polymer/layered silicate, Polymer/CNT, Polyester/TiO ₂

From the past few decades polymeric nanocomposites have been extensively synthesized and studied for the various properties such as optical properties, thermal properties and flame retarding properties [7-9].

1.3. Properties of Polymeric Nanocomposites

The transition of particle dimension from micro scale to nano scale resulted in enhancement of various properties.

1.3.1. Dielectric Properties

Dielectrics are the materials having permanent electric dipole moment. They are electrical insulators and can be used to store electrical energy. Polymeric nanocomposites having high dielectric constant and low dielectric loss is used in capacitors and other electronic circuits. Incorporation of noble metal nanoparticles as nanofillers in polymers enhances the dielectric constant of polymer and reduces the dielectric loss e.g polyaniline/silver nanocomposites possess dielectric constant and dielectric loss of 5.8 and 0.023 at 2.5 mol % of silver nanoparticles respectively. The better dielectric loss makes PANI/Ag nanocomposites as better matrix to store electric potential energy under the influence of alternative electric field [10]. Copper nanowires/poly (vinylidene fluoride) nanocomposites also possess lower dielectric loss with better performance as charge storage applications [11]. Polymer ceramic nanocomposites also found application in embedded capacitor materials. Combination of

lead magnesium niobate-lead titanate as ceramic filler in epoxy matrix enhances the dielectric constant to much higher values. TiO_2 , ZnO and Al_2O_3 at low filler loading in epoxy matrix also result in low value of dielectric loss. Comparison of values of dielectric loss of nanocomposite system with microcomposite shows that microcomposites of respective oxide exhibit higher values than nanocomposites which limit its use in electronic circuits [12-13].

1.3.2. Mechanical Properties

Addition of nanofillers also improves the mechanical strength, storage modulus, young's modulus and flexural modulus of resulting nanocomposite. Polymer clay nanocomposites are found to exhibit excellent mechanical strength. Caprolactam-nylon clay hybrid with uniformly dispersed silicate layers of montmorillonite possess higher tensile modulus and heat distortion temperature at higher montmorillonite content [14]. Homogenous dispersion combined with the interfacial interaction of graphene at low filler content with polyvinyl alcohol causes increase in modulus up to 212 Nm^{-2} compared with pure polyvinyl alcohol [15].

1.3.3. Thermal Properties

Polymeric nanocomposites possess high dielectric constants but only few reports have been made on material possessing both high dielectric constant and high thermal properties. High voltage industries and microelectronics focus the use of material having increased cooling rate that is brought about by the use of materials with high thermal conductivity. Poly (vinylidene fluoride) composites filled with silver metal nanoparticles resulted in improved thermal conductivities. At filler loading of 20 wt % value of thermal conductivity reported is 6.5 W/mK [16].

1.4. Applications of Polymeric Nanocomposites

Polymeric nanocomposites are extensively synthesized and exhibit much advanced applications. Few of the common applications are summarized below.

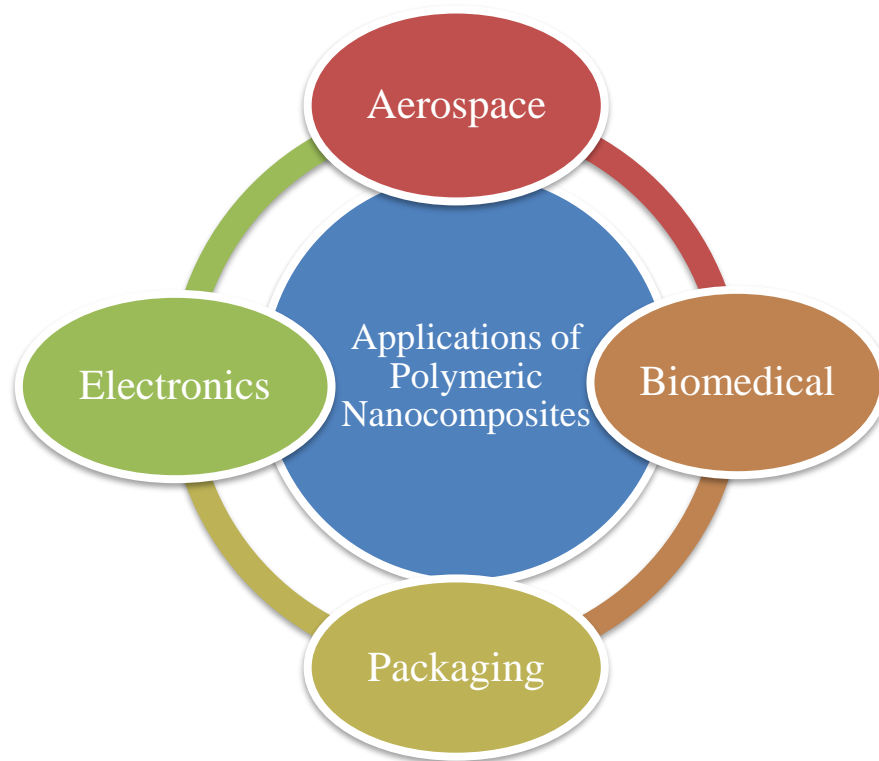


Figure 1.2: Applications of polymeric nanocomposites.

1.4.1. Electronics

Electronic devices have deep embedded design of nanotechnology. The applications of polymeric nanocomposite in field of electronics is quite diverse and have been proposed for various application in chemical sensors, batteries , memory devices, photodiode photoelectric cells LED [17].

1.4.2. Aerospace

Based on enhanced tensile strength, thermal conductivity, durability and improvement in various mechanical properties focused the use of polymeric nanocomposite in aerospace industry. Increased in the modulus of elasticity and improved mechanical properties is observed by the dispersion of multiwall carbon nanotubes as a nanofillers in epoxy matrix because of strong adhesion between the polymer and nanofillers [18].

1.4.3. Biomedical

Biomedical researcher focused now day on the use of polymeric nanocomposites as biomedicine because of their effectiveness. Graphene and carbon nanotubes based polymeric nanocomposite hydrogels are potential source of applications such as conductive tapes, actuators, drug delivery system and biomedical devices [19]. Interaction of nanocarriers with the cell membrane resulted in the uptake of drug by endocytosis. Water soluble PEGylated nanographene oxide is found to be very potent drug for killing invitro cancer cell line in human colon and exhibits 1000 folds more potency than other drugs [20]. Increase in permeability of tumor vasculature to macromolecule is facilitated by passive targeting of tumor cell by polymeric carriers e.g. Peripheral modification of polylysine based dendrimers is promising vaccine for antiviral and antibacterial infections [21].

1.4.4. Packaging

No material is completely impermeable to atmospheric gases or water. Nylon-6 nanocomposites are known to have better barrier properties to gas and water and have excellent transparency [22]. Non-degradable packaging materials are causing serious global environmental pollution. Homogenous dispersion of montmorillonite nanoparticles in starch based material resulted in the formation of biodegradable starch/clay nanocomposite films that are used for packaging and helps in the reduction of biomass accumulating on the earth [23].

1.5. Characterization Techniques

The structure, size, composition, morphology and various properties of prepared samples have been studied by various characterization techniques. The brief description on instrumentation and principle of these techniques are described in next section.

1.5.1 X-ray Diffraction

X-ray powder diffraction is the analytical technique used to reveal structural information such as chemical composition, Bravais lattice symmetry, lattice parameter of unit cell, crystal structure, layered thickness and crystallite size.

1.5.1.1 Fundamental Principle

The fundamental principle lying behind the X-ray diffraction is “Production of constructive interference at specific angles due to diffraction that occur when light is scattered by periodic array with long range order.”

The periodic array of atom in crystal causes the light to diffract from various crystalline planes. The wavelength of X-ray must be similar to the distance between the atoms. The scattering of X-ray from the atoms produces a diffraction pattern, providing information about the atomic arrangement within the crystal. An X-ray reflected from the surface of the crystal has travelled less distance than that reflected from plane of atom inside the crystal. The penetrating X-ray travels down to the internal layer, reflect, and travel back over the same distance before coming back at the surface. The distance travelled by the X-ray depends on the separation of the layers and angle at which the X-ray entered the material. The position of the diffraction peaks are determined by the distance between the parallel planes of atom. The diffraction of X-ray by the crystal is described by the Bragg's law.

$$2d\sin\theta = n\lambda$$

Where d is the spacing between the diffracting planes, θ is the angle between the incident ray and layers of crystal, n is whole number integer, λ is the wavelength of the incident X-ray beam.

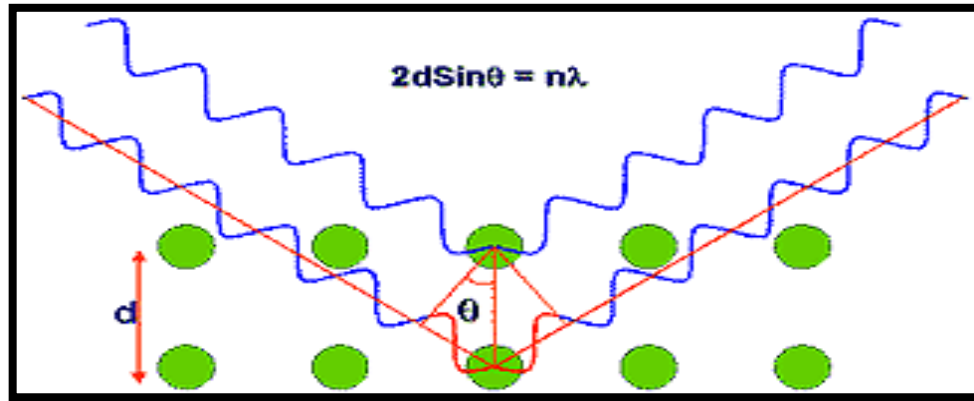


Figure 1.3: X-ray diffraction.

1.5.1.2 Instrumentation of X-ray Powder Diffraction

The X-ray powder diffractometer consists of

- X-ray tube
- Sample stage
- X-ray detector
- **X-ray tube**

The most common source of X-ray is the X-ray tube. The tube is evacuated, contains copper block with metal target anode and a tungsten filament cathode.

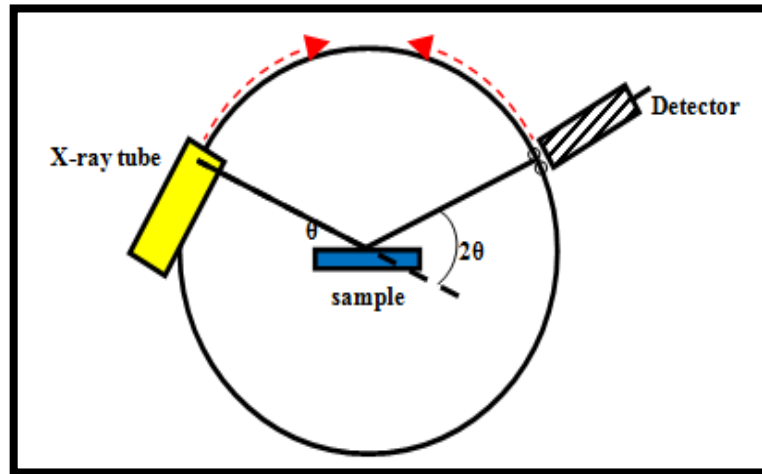


Figure 1.4: X-ray diffractometer.

- **Sample stage**

The sample to be analyzed is placed on the sample stage of X-ray diffractometer and irradiated with the X-rays.

- **X-ray detector**

X-ray detector or transducer in the modern equipments, produces electrical signal when exposed to the radiation. These detectors are often used as photon counters, so intensities are determined by the number of counts in a certain amount of time. Monochromatic X-rays helps in the determination of interplanar spacing of unknown materials. Analysis of sample is done in powder form with grains in the random orientations to insure that all crystallographic directions are “sampled” by the beam. When the Bragg conditions for constructive interference are obtained, a "reflection" is produced, and the relative peak height is generally proportional to the number of grains in a preferred orientation.

1.5.2 Scanning Electron Microscopy

Scanning electron microscope involves the production of image of sample by scanning the surface with the beam of electron. Interaction of electron with the atoms of sample

results in producing various signals that contain information about sample's surface topography and composition.

1.5.2.1 Working of SEM

Electron gun present at the top of microscope produces a beam of electron. This beam of electron follows the vertical path through the microscope, held within the vacuum. The beam travels through electromagnetic fields and lenses that focus the electron beam toward the sample. Once the beam of electron hits the sample, ejection of electron and X-rays from the sample takes place.

1.5.2.2 Fundamental Principle of Scanning Electron Microscopy

The significant amount of energy is carried by accelerated electron in SEM. Electron-sample interaction resulted in dissipation of this energy and produce various signal as electron are decelerated in solid sample. These signals include secondary electrons, backscattered electron (BSE), diffracted backscattered electrons, photons, visible light and heat. Secondary electrons are most valuable for showing morphology and topography on sample while back scattered electrons are responsible for illustrating contrasts in composition in multiphase sample. Inelastic collision of electrons with electrons in the discrete orbital's of atom in sample results in the generation of X-rays. As the excited electron returned to the lower energy state they yield X-rays of same fixed wavelength. Thus characteristics X-rays are produced for each element. SEM analysis is considered to be nondestructive. So it is possible to analyze the same sample repeatedly.

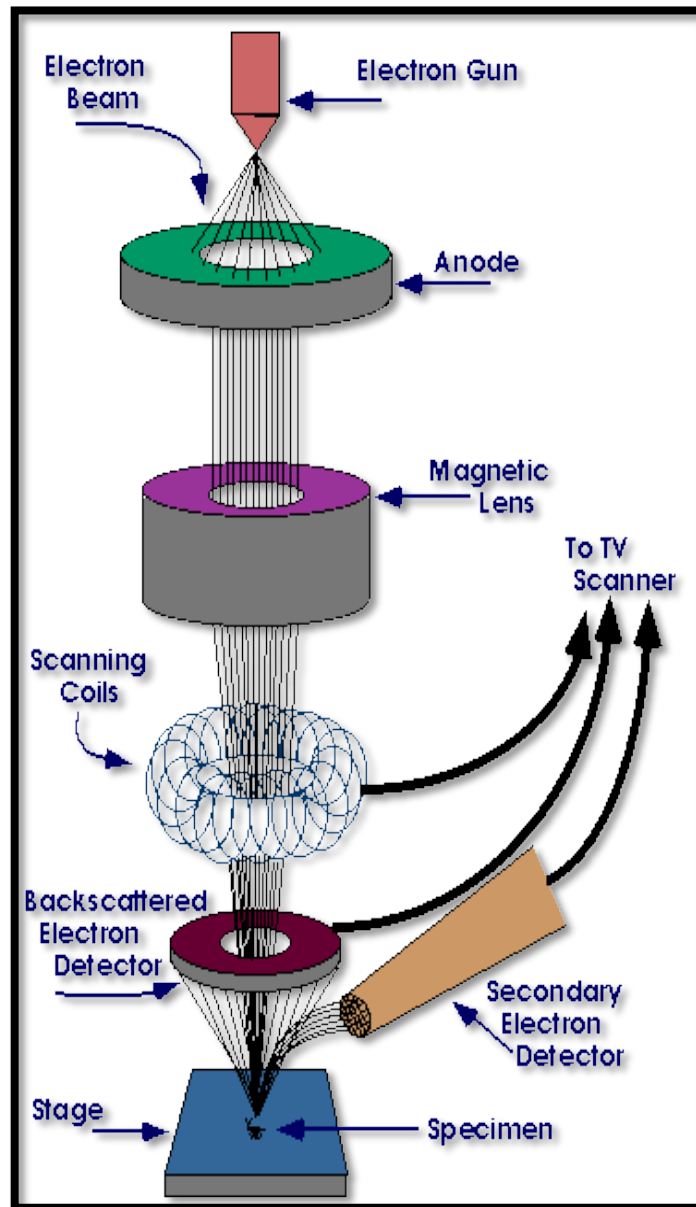


Figure 1.5: Schematic diagram of SEM.

1.5.2.3 Instrumentation of SEM

Instrumentation of scanning electron microscope includes

- Electron gun
- Electron lenses
- Sample stage
- Detectors
- Display / Data output devices.

- **Electron gun**

Electron gun produce steady beam of electron. Electrons are produced either by Thermionic emission i.e. apply thermal energy to coax electron from tungsten filament or by Field emission i.e. apply strong field to pull electron away from atom.

- **Electron lenses**

The electron lenses in SEM produces convergent electron beam with desired crossover diameter. These metallic lenses have cylindrical hole, which operate in vacuum. Magnetic field is generated inside these lenses, which in turn is varied to focus or defocus the electron beam passing through the hole of the lens.

- **Sample stage**

The place where sample is placed is called sample stage.

- **Detector**

- a) **Secondary electron detector**

Inelastic interaction of primary electrons with the electrons in the K shell of atom of sample material resulted in the emission of secondary electron. Secondary electron imaging produced by secondary electron detector (SED) has greater resolution and provides topographical information of sample. The image of SED exhibits resolution independent of material. The construction of SED is shown in the diagram below

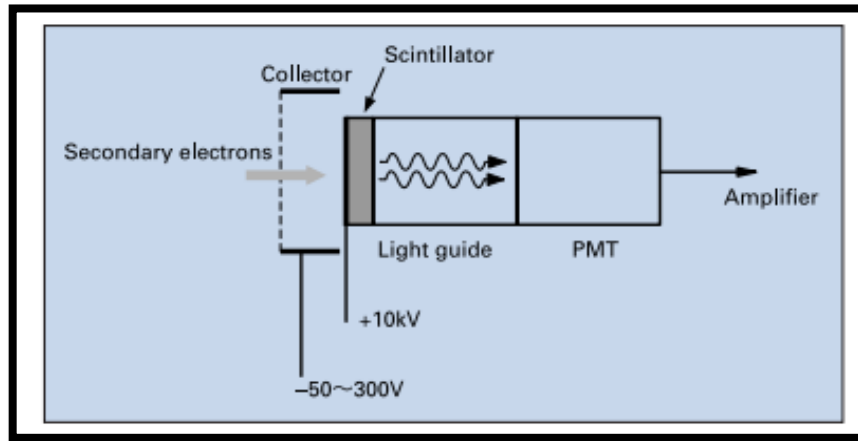


Figure 1.6: Secondary electron detector.

A supplementary electrode called the collector applies high voltage of 10 kV to scintillator (fluorescent substance) causing the emission and attraction of secondary electron from the sample material towards the scintillator. The light is generated upon the collision of electrons with the scintillator. The light then is converted into electrons which are amplified as an electric signal.

b) Backscattered electron detector

A backscattered electron detector (BSD) detects elastically scattered electron. Heavier atoms produced more backscattered electrons (BSE) and results in higher signal as compared to lighter atoms. This dependence of BSE on atomic number “Z” helps us to differentiate between different phases. A BSE image provides valuable information related to sample’s composition, topography, crystallography and magnetic field of sample material.

- **Display/Output devices**

The output signal from secondary electron detector is sent to the liquid crystal display (LCD) unit after amplifying it. The electron probe changes its scan speed in several

steps; Fast scan rate is used for observation while slow scan speed helps in acquisition to save various images.

1.5.3 Infrared Spectroscopy

Infrared spectroscopy involves the interaction of infrared radiations with matter. The infrared portion of electromagnetic portion is divided in to three regions the near-, mid-, and far infrared region. The mid-infrared, approximately $4000\text{--}400\text{ cm}^{-1}$ is used to study the fundamental vibrations and associated rotational-vibrational structure.

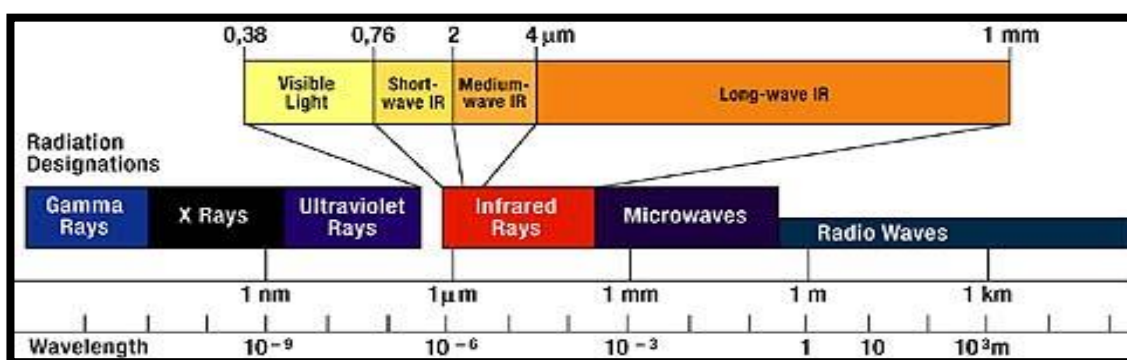


Figure 1.7: Electromagnetic radiation spectrum.

1.5.3.1 Principle

Infrared spectroscopy is based on the absorption of radiation and then vibration of molecule and by utilizing this technique various functional groups present within the molecule is determined. Absorption of radiation by molecule involves increase in the energy that in turns is directly proportional to light absorbed. In IR spectroscopy polychromatic light is passed through a sample and intensity of transmitted light is measured at each frequency. Absorption of IR radiation leads to the transition of molecule from ground vibrational state to excited vibrational state as shown in figure.

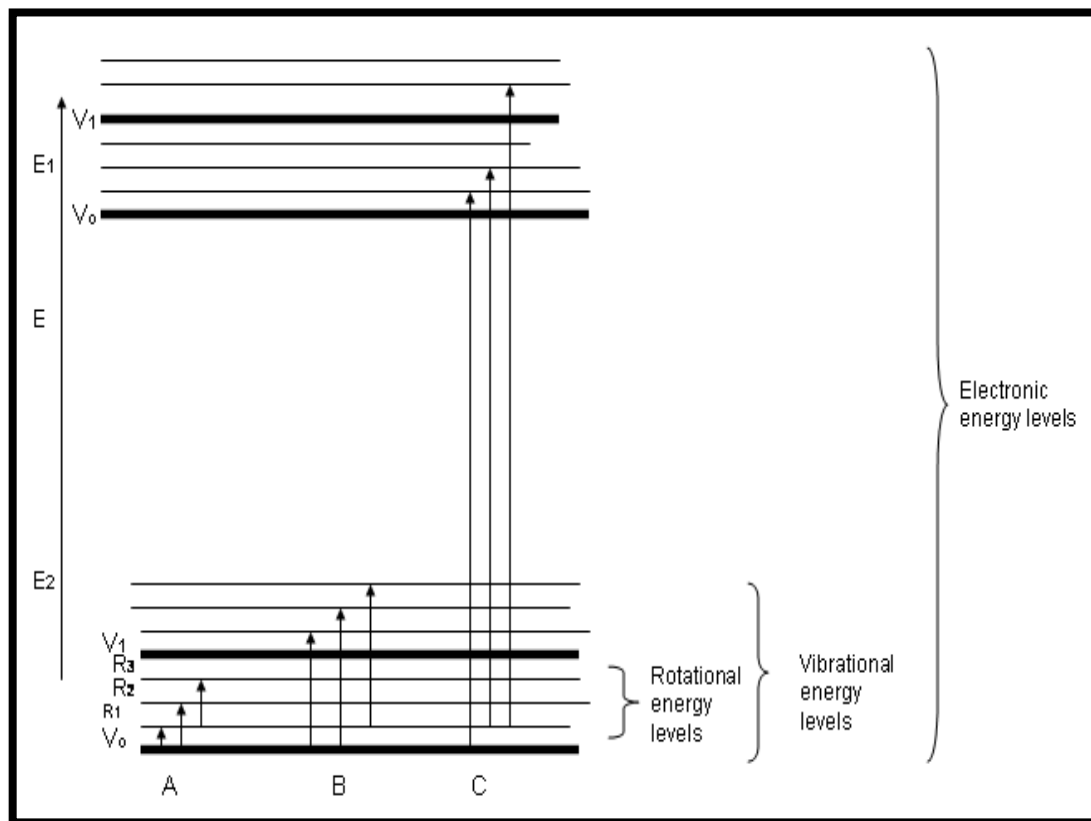


Figure 1.8: Energy levels in IR.

When IR radiations are absorbed, IR active molecules undergo change in the dipole moment. The dipole moment changes as bond contract and expand. The vibrational frequency of molecule can be calculated by the formula

$$\bar{\nu} = \frac{1}{2\pi c} \sqrt{k/\mu}$$

Where “c” is the speed of light, “k” is the force constant and “ μ ” is the reduced mass.

1.5.3.2 Instrumentation

An infrared spectrophotometer is an instrument that produces infrared spectrum of a molecule by passing infrared light and spectrum is plot of amount of radiations

transmitted (y-axis) against wavelength of infrared radiations (x-axis). IR spectra provide considerable amount of data about the structure of compound. The main parts of IR spectrophotometer are

- Radiation source
- Sample cell
- Monochromator
- Detectors
- Recorder

- **Radiation source**

Radiation source emit IR radiations intense enough for detection and extend over desired wavelength. IR radiation sources are Nernst glower, Nichrome wire, Mercury arc, Glycer source, tungsten lamp and incandescent lamp.

- **Sample cell**

Sample cell contain sample which may be either solid in the form of pellet, solid film or in liquid form dissolved in chloroform or in gas form.

- **Monochromator**

Monochromator disperses IR beam. Most commonly used monochromator are prism, gratings and prism.

- **Detectors**

Detectors are used to measure the intensity of transmitted infrared radiations. Detectors like thermocouples, thermistors and pyro-electric detectors are used.

- **Recorder**

Recorders are used to record the spectra of compound.

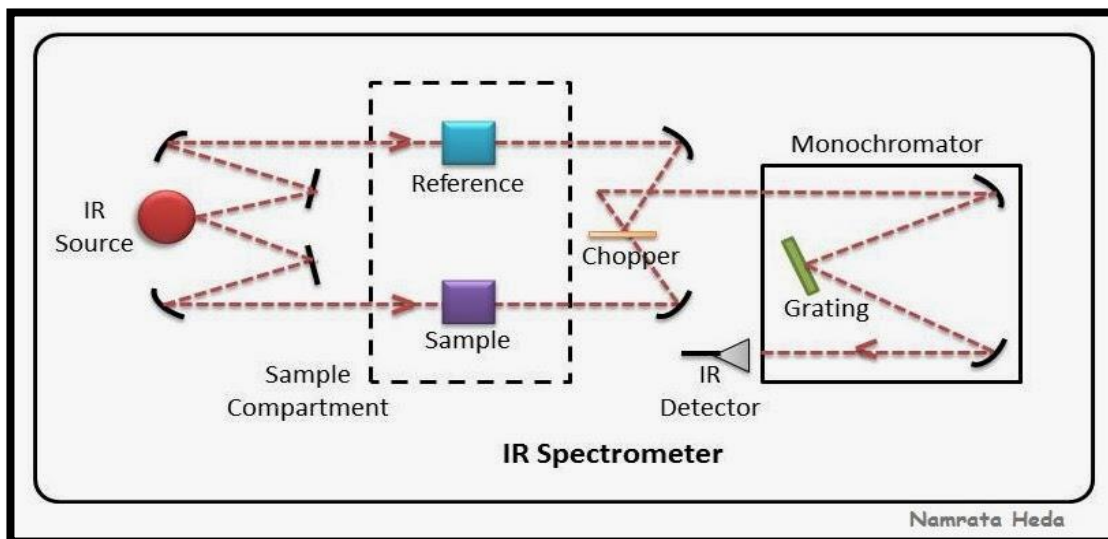


Figure 1.9: Instrumentation of IR spectrometer.

1.5.4 LCR Meter

An instrument usually employed to find inductance (L), capacitance (C), and resistance (R) of electric devices is called LCR meter.

➤ Inductance

Inductance is the property of electric circuit defined as “variation in current flowing in circuit itself or the neighboring circuit causes the generation of electromotive force”. Inductance is measured in henry (H) equals to kilogram meter square per second square per ampere square ($\text{Kgm}^2\text{s}^{-2}\text{A}^{-2}$)

➤ Capacitance

Capacitance is ability of system to store electric charge, defined as “ratio of change in electric charge to corresponding electric potential change”. Unit of capacitance is farad (F) i.e. one coulomb per volt (CV^{-1}).

➤ **Resistance**

Resistance is defined as “opposition to the flow of electric current” and it is measured in ohms that is equal to volt per ampere (VA^{-1})

1.5.4.1 Fundamental Principle and Working of LCR Meter

Two commonly used technique for LCR meter is Bridge method and Current-voltage method.

a) Wheatstone bridge method

This method uses balanced bridge. Positions of bridge component at the balance point can the value of test component. Lower frequency measurement, frequencies up to 100 kHz is used for this method. Its construction consist of four resistors, two resistors with known impedance Z_2 and Z_4 , one variable resistor Z_1 while unknown resistor (DUT) is also placed in the bridge is represented by Z_u . Z_1 is changed until current flow through M becomes zero. At this point ratio of known resistors Z_4 and Z_2 becomes exactly equal to ratio of adjusted value of variable resistor Z_1 and unknown resistor Z_u . This balance position of bridge shows that four resistor in the circuit obeys equation given below.

$$Z_u = \left(\frac{Z_4}{Z_2}\right) Z_1$$

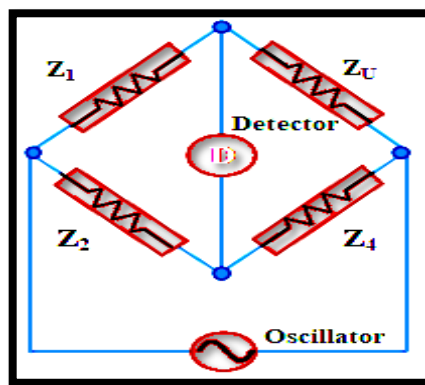


Figure 1.10: Circuit diagram for Wheatstone bridge method.

b) Current-voltage measurement

Highly accurate measurements used for higher frequency application and over wide range of values are determined by current-voltage approach. This approach measure current as well as voltage. The frequencies involved are high so it uses impedance matched measurement circuit. Low impedance and high impedance current-voltage LCR meter have two types of voltmeter and current meter, one for each arrangement. Using voltage and current values from the measurement, impedance can be calculated. Relative phase of current and voltage by the use of phase sensitive detector can be used to measure resistance, conductance and inductance of the sample under examination.

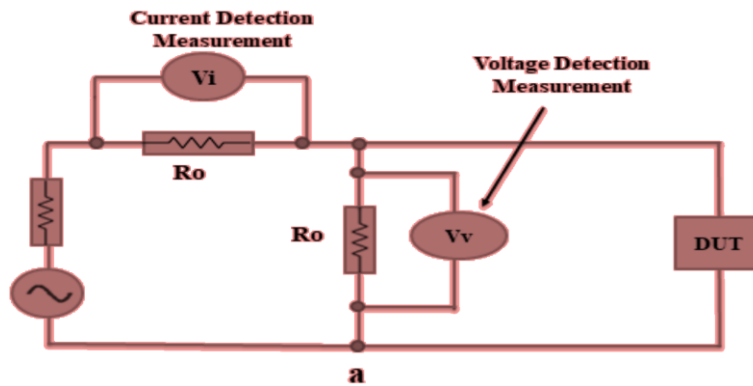


Figure 1.11: Circuit diagram for LCR meter at low voltage.

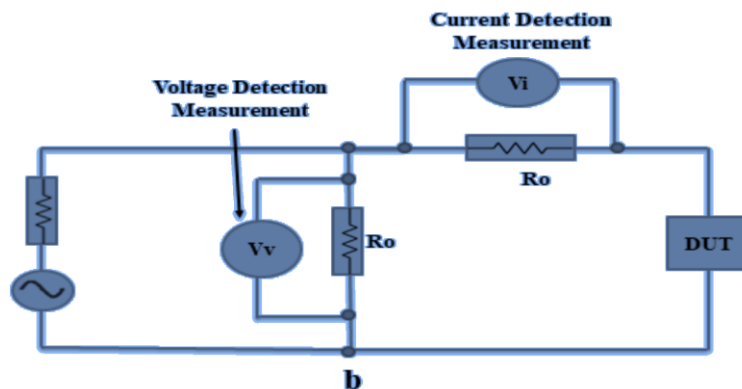


Figure 1.12: Circuit diagram for LCR meter at high voltage.

Chapter 2

Literature Survey

2.1. Copper Nanoparticles

Copper is d-block transition metal having atomic mass 63.5, atomic number 29 and possess electronic configuration of $3d^{10} 4s^1$. It is soft, malleable and ductile with high electrical and thermal conductivity.

2.1.1. Synthesis of Copper Nanoparticles

Copper nanoparticles have tendency to undergo agglomeration and oxidation when exposed to air. These problems are avoided either by carrying out synthesis in organic phase [24], in an inert gas atmosphere [25], by the use of protective polymer [26] or carrying out synthesis in the presence of surfactant [27]. Copper nanoparticles are synthesized by various methods. The most commonly used methods are chemical reduction [28-29], sonochemical reduction [30], gamma radiations [31], laser ablation [32], microwave assisted [33-34], green synthesis [35-36], reverse micelles [37] and polyol method [38-40].

Copper nanoparticles was first synthesized by Pileni et al. in 1993 by reverse micelles method using copper dioctyl sulfosuccinate ($\text{Cu}(\text{AOT})_2$) and reducing agent hydrazine (N_2H_4) and sodium borohydride (NaBH_4) [41]. Polyol method was first developed by Fernand et al. in 1993 but the synthesis includes the particle size in micrometer range [42]. Synthesis of copper nanoparticles by using polyol solvent along with microwave radiations was introduced in 2004 by Zhu et al. typical procedure for the synthesis includes dissolution of copper sulphate pentahydrate ($\text{CuSO}_4 \cdot 5\text{H}_2\text{O}$) in ethylene glycol (EG), addition of Polyvinylpyrrolidone (PVP) as protecting agent in above solution and

then placing it on magnetic stirring, reducing agent sodium phosphinate monohydrate ($\text{NaH}_2\text{PO}_2 \cdot \text{H}_2\text{O}$) dissolved in EG is added to the above solution, after that mixture is placed in microwave oven for 5 min. The change in the color of mixture from light blue to dark black results in the formation of copper nanoparticles [43]. In 2006 Cha et al. synthesized copper nanocrystals by polyol method using copper acetylacetonate ($\text{Cu}(\text{acac})_2$) as copper source, 1, 2-hexadecandiol as polyol reducing agent, octyl ether as solvent and in the presence of surfactants oleylamine, trioctylphosphine oxide and oleic acid [44]. In next year polyol method was also used by Park et al. $\text{NaH}_2\text{PO}_2 \cdot \text{H}_2\text{O}$ is added to the solution of PVP in diethylene glycol (DEG) and solution is heated at 200 °C. Aqueous solution of $\text{CuSO}_4 \cdot 5\text{H}_2\text{O}$ is prepared and added to the reaction mixture by syringe pump. The use of nonaqueous solvent as a reaction medium minimizes the surface oxidation [40]. Tooba et al. in 2008 synthesized nanosized copper powder by polyol method using copper acetate monohydrate ($\text{Cu}(\text{acetate})_2 \cdot \text{H}_2\text{O}$) as precursor salt taken in three necked flask having magnetic stirrer, adding EG that act both as solvent as well as reducing agent and heating reaction mixture to 200 °C [45]. In 2011 Carroll et al. used hydrated metal precursor salt with polyol liquid along with sodium hydroxide (NaOH). Refluxing and distilling the reaction mixture for two hour leads to the formation of copper nanoparticles of different morphologies [46]. EG based copper nitrate trihydrate ($\text{Cu}(\text{NO}_3)_2 \cdot 3\text{H}_2\text{O}$) and PVP solutions were prepared. Equal volume of both solutions were stirred together and heated in autoclave for 30 h. Reddish brown precipitate obtained were washed with DI water and centrifuged [39].

2.1.2. Application of Copper Nanoparticles

Copper nanoparticles exhibit various useful applications. Copper nanoparticles are found to be very effective catalyst showing yield up to 88 % in condensation of iodobenzene to biphenyl i.e. Ullmann Reaction [30]. Recyclable PVP protected nanoparticles are subjected as catalyst for cycloaddition reaction between several azides and terminal alkynes [47]. Copper also exhibits antimicrobial performances. Copper nanoparticles

interact with the microbial cell membranes and exert the promising antibacterial activity against Gram positive and Gram negative bacteria [48]. Copper nanoparticle cationized empty fruit bunch fiber shows sterilization of *E.coli* and *S. aureus* bacteria hence copper nanoparticles are considered to be the potential biocide [49]. 2, 3-bis-[(3-ethoxy-2-hydroxybenzylidene) amino] but-2-enedinitrile copper complex shows activity against cancer cell lines. This cytotoxic activity would help the research for the future use of copper nanoparticles as a cytotoxic drug [50]. Copper nanoparticles show resistance in triboelectric charging i.e. ability to dissipate electrostatic charges. This antistatic property is basically measure of electrical resistance. This property makes the use of copper nanoparticles in capacitors [48]. The conductive nature of copper makes the use of copper nanoparticles in printed electronics thus are potential for replacing expensive silver ink that were previously used. The conductive copper nanoparticle ink has long term oxidative stability and dispersive stability [51- 53].

2.1.3. Synthesis and Properties of Copper based Polymeric Nanocomposites

Karkov in 2001 prepared the copper-polyethylene nanocomposites involving synthesis of copper nanoparticles by decomposing $\text{Cu}(\text{acetate})_2 \cdot \text{H}_2\text{O}$ and adding the solution of it in high-temperature solution of polyethylene matrix dissolved in vacuum oil [54]. Akamatsu et al. demonstrated a new methodology of preparing monodispersed copper nanoparticles in polyimide resins. Synthesis includes the immersion of films of pyromellitic dianhydride-oxydianiline (PMDA-ODA) in aqueous KOH and then washing with the distilled water. In next step, films are then immersed in aqueous copper sulphate solution for the exchange of potassium ion with copper ion, washed with distilled water then dried. Annealing of films was done under nitrogen at various temperatures [5, 55]. Cioffi et al. electrosynthesized the copper nanoparticle in the presence of tetraoctyl ammonium salt dissolved in acetonitrile/tetrahydrofuran (THF). The composite was prepared by mixing colloids of copper with the solution of poly-

vinyl-methyl- ketone [56]. The synthesis of copper-polypropylene and their antibacterial properties was reported by Plaza et al. High content nanoparticles bearing composites were found to be very effective against the strains of bacteria showing reduction in killing time [57]. Copper-polystyrene nanocomposite was *ex-situ* synthesized by Kamrupi et al. in 2009 and also studied the antimicrobial properties of prepared nanocomposite. Copper nanoparticles are prepared by reducing CuCl_2 with the NaBH_4 . Styrene monomer is dissolved in doubled-distilled water solution of PDMS-AIBN with vigorous stirring to achieve pre emulsion. Addition of varied concentration of copper nanoparticles in prepared monomer solution and allowing the polymerization resulted in formation of nanocomposite. Among the four bacterial strains on which antimicrobial activity was tested *Bacillus circulens* was very sensitive toward the Cu-encapsulated polystyrene nanocomposite particles [58]. Tian *in-situ* synthesized copper nanoparticles in polystyrene matrix. Copper nanoparticles were synthesized by the reduction of cupric sulfate with the hydrazine hydrate in the presence of PVP and cetyltrimethyl ammonium bromide (CTAB) which are then introduced in the matrix of polystyrene by *in-situ* emulsion polymerization [59]. In next year well dispersed copper nanoparticle in polyacrylonitrile (PAN) nanofibers was prepared by Xu et al. by electrospinning and high pressure hydrogenation technique. Dimethyl formamide (DMF) is used to dissolve the polyacrylonitrile, $\text{Cu}(\text{NO}_3)_2 \cdot 3\text{H}_2\text{O}$ is added to the solution and solution have to undergone the electrospinning procedure at room temperature. The obtained $\text{Cu}^{+2}/\text{PAN}$ nanofibers undergo high pressure hydrogenation [60]. A Guzman et al. used the two methods i.e. *in-situ* and *ex-situ* synthesis of copper nanoparticles in the polyvinyl chloride (PVC). *Ex-situ* synthesis of copper nanoparticles is carried out by using polyol method involving use of anhydrous $\text{Cu}(\text{acetate})_2$ as a precursor salt, ascorbic acid and PVP both are separately dissolved in the ethylene glycol and mixed, solution formed is stirred, heated at constant reflux undergo microwave heating then $\text{Cu}(\text{acetate})_2$ dissolved in EG is added, Cu^{+2} undergo reduction, copper nanoparticles formed are centrifuged

and washed. *In-situ* synthesis of copper nanoparticles is carried out by adding the salt copper acetate, reducing agent ascorbic acid (AA) and PVP in the stabilizing solvent DOP, heating the reaction mixture and then adding PVC resin to get fine dispersion of formed nanoparticles within the polymeric matrix [61]. Safiullah et al. in the same year *in-situ* synthesized the copper nanoparticles within the matrix of poly (Glycidyl methacrylate) (PGMA). For the synthesis of PGMA, in the solution of surfactant polyvinyl alcohol (PVA), monomer glycidyl methacrylate, initiator benzoyl peroxide, disodium hydrogen phosphate is added and placed for stirring under nitrogen. The solution was filtered; solid product was washed and dried to obtain spherical beads of PGMA. Cu-PGMA nanocomposite was *in-situ* synthesized via suspension polymerization. The sol is prepared by dissolving the $\text{CuSO}_4 \cdot 5\text{H}_2\text{O}$, AA and polyethylene glycol in water and then adding this sol along with NaBH_4 in PGMA matrix [62]. In a very next year composite membrane of poly (vinylidene fluoride) (PVDF) with organoclay stabilized copper nanoparticles was prepared and characterized. *Ex-situ* synthesis of organoclays stabilized copper nanoparticles is carried out in the presence of organoclays and N_2 atmosphere, and by reducing $\text{CuSO}_4 \cdot 5\text{H}_2\text{O}$ with NaBH_4 . Synthesis of composite membrane involves dissolution of PVDF in dimethyl acetamide (DMAc) under continuous stirring and addition of copper nanoparticles in solution. Phase inversion method then helped in the casting of composite membrane [63]. Nathiya et al. synthesized and studied the anticancerous, antimicrobial and photocatalytic activity of the chitosan-copper (CS-Cu) nanocomposite. Synthesis includes the addition of 1 % chitosan in solution of acetic acid (CH_3COOH) and sodium chloride (NaCl) which is stirred overnight to dissolve the chitosan. Add $\text{CuSO}_4 \cdot 5\text{H}_2\text{O}$ to above viscous solution and continue stirring for 24 h. The mixture is centrifuged, residue is filtered, washed and dried in oven at $80\text{ }^\circ\text{C}$ for 5 h. CS-Cu nanocomposite was found effective against the five strains i.e. two gram positive bacteria, two gram negative bacteria and one fungal. The

CS-Cu nanocomposite is seemed to exhibit 50 % inhibition in biological activity of cancer cell [64].

2.1.4. Synthesis of Poly (vinyl chloride-co-vinyl acetate-co-vinyl alcohol) based Nanocomposites

Nadeem et al. in 2010 by using sol gel technique synthesized the co-poly (vinyl chloride-vinyl acetate-vinyl alcohol) silica nanocomposites and have studied the optical, mechanical and thermal properties. Synthetic process includes the preparation of stock solution of copolymer in dried THF. Mixing of appropriate amounts of copolymer along with the various concentrations of tetraethyl orthosilicate results in hybrid formation. Hydrolysis and condensation is carried out by adding aqueous solution of THF and triethylamine as a catalyst in hybrid solution. Transparency of thin films decreases and films become opaque as silica content reaches up to 10 %. Mechanical properties revealed that modulus is increased only for the system containing 2.5 % silica relative to the pure polymer while decrease in the stress strain ratio is seen for the rest of the systems [65]. Benounis et al. synthesized the phosphate selective poly (vinyl chloride-co-vinyl acetate-co-vinyl alcohol) membranes of different composition. Chromoionophore 4, 5-dibromo-fluorecein-octadecylester $C_{38}H_{46}Br_2O_5$ and ionophores trioctyl-tin chloride and methylenebis [dibromo (phenyl) stannane] are used as plasticizers and added to copolymer poly (vinyl chloride-co-vinyl acetate-co-vinyl alcohol) in 1:2 ratios. The solution in THF is prepared to get the membranes. The application of these membranes as a phosphate sensor is conducted on real water and result showed that membranes having low plasticizers are highly selective toward hydrophilic phosphate anion [66].

Chapter 3

Experimentation

3.1 Experimental Work

The experimental work includes synthesis of copper nanoparticle by modified polyol method and preparation of thin films of poly (vinyl chloride-co-vinyl acetate-co-vinyl alcohol)/copper nanoparticles by solution casting method.

3.1.1 Polyol method for Copper Nanoparticle Synthesis

- **Modified Polyol Method**

A polyol is an alcohol having two or more hydroxyl groups. Polyol are considered to be water equivalent showing solubility of compounds similar to water. Polyol are excellent reducing agent for noble metal precursor without need of additional reducing agent [67]. The metal precursor salts such as sulfate, acetate, nitrate, chloride or hydroxide is suspended in polyol liquid such as ethylene glycol (EG), diethylene glycol (DEG) or tetraethylene glycol (TEG) etc. After dissolution and adding capping or dispersing agent, solution is heated between 180-200 °C. Reduction and nucleation result in fine nanoparticles. In modified polyol method polyol liquid such as ethylene glycol is used not only as a solvent but also as a reducing agent [68]. Polyvinylpyrrolidone is used as capping, dispersing or protecting agent prevents the surface oxidation of copper nanoparticles. The reduction proceed via a solution rather than solid phase so metal particles are formed by nucleation and growth from the solution [69].

The polyol method is

- Simple and effective
- Have low cost and high yield

3.1.2 Synthesis of Copper Nanoparticles

A very simple and environmentally friendly method is used for the synthesis of copper nanoparticle. The details of chemicals utilized in the synthesis of nanoparticles are given in the table below.

Table 3.1: List of chemicals used in the synthesis.

S. No	Chemicals	Chemical Formula	Molecular Weight	Company	Purity %
1	Copper hydroxide	$\text{Cu}(\text{OH})_2$	97.56	Aldrich	99
2	Polyvinylpyrrolidone (PVP)	$(\text{C}_6\text{H}_9\text{NO})_n$	40,000	CalbioChem	99
3	Ethylene Glycol (EG)	$\text{OH}(\text{CH}_2)_2\text{OH}$	62.07g/mol	Merck Millipore	99

In synthesis of copper nanoparticles 4 g of copper hydroxide ($\text{Cu}(\text{OH})_2$) is dissolved in 80 mL of ethylene glycol in a beaker, 4 g polyvinylpyrrolidone is added in the solution above and keep the solution on stirring at room temperature to get a homogenous mixture. After getting the homogenous blue coloured mixture, the solution is heated at 200 °C with continuous stirring for 2 h. The ethylene glycol evaporates resulting in the formation of reddish brown color precipitates that are crushed to get fine powder of copper nanoparticle.

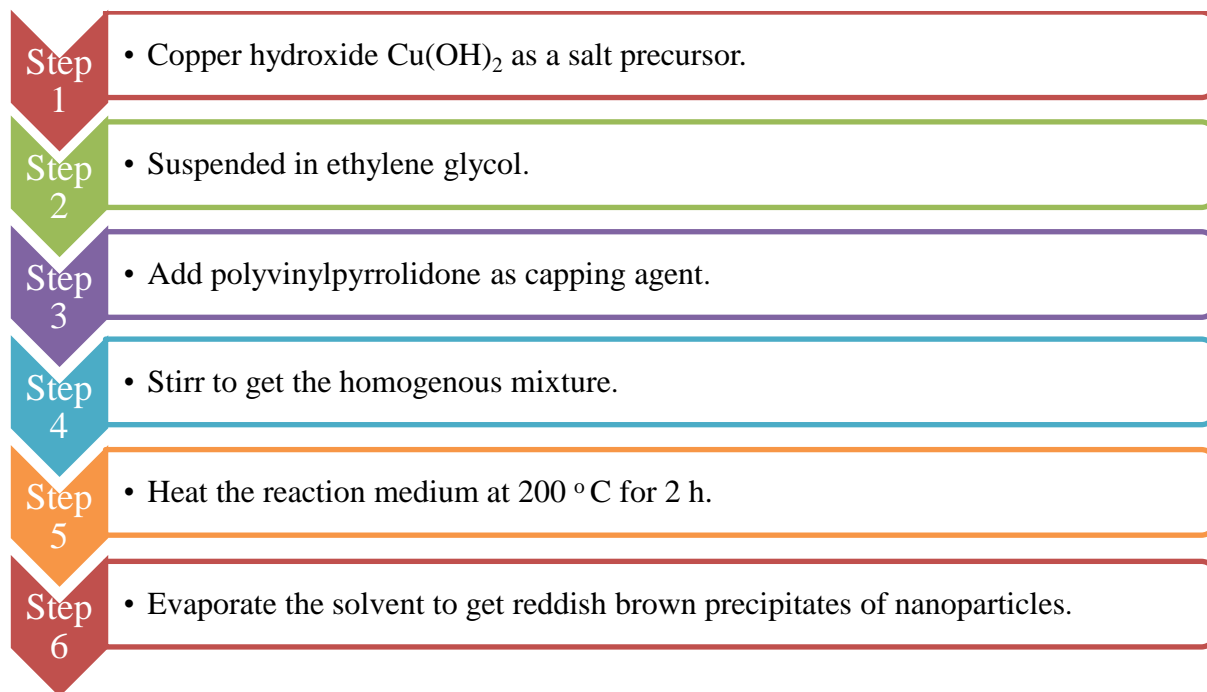
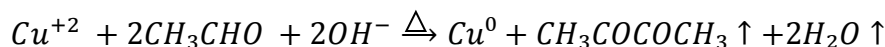
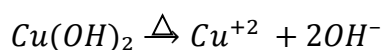
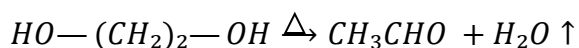


Figure 3.1: Graphical representation of synthesis of Copper nanoparticles.

3.1.3 Mechanism of Reaction

The mechanism of described procedure is as under



Overall reaction is



High temperature results in the decomposition of ethylene glycol into acetaldehyde and provides electrons for the reduction of Cu^{+2} to Cu^0 and cause oxidation of acetaldehyde into diones. Copper nanoparticles synthesis by using $\text{Cu}(\text{OH})_2$ as precursor salt avoids impurities like SO_4^{-2} and Cl^- that are produced by using other salt precursors. Reducing

agents like hydrazine and sodium borohydride are toxic to environment unlike the ethylene glycol that is environmentally friendly. The function of PVP is to protect the surface oxidation of nanoparticles and disperse them [70].

3.1.4 Synthesis of PNCs Thin Films

Chemicals used for the synthesis of polymer films are given below in the table.

Table 3.2: List of Chemicals used in the synthesis of thin films.

S. No	Chemicals	Molecular weight	Tg	Company	Purity %
1	Polyvinyl Chloride-co-Polyvinyl Acetate-co-Polyvinyl Alcohol	27,000	76 °C	Aldrich	99
2	Tetrahydrofuran	72 g/mol	–	Aldrich	99

Poly (vinyl chloride-co-vinyl acetate-co- vinyl alcohol) has average molecular weight of 27,000. The composition of polymer is polyvinyl chloride 90 wt %, polyvinyl acetate 4 wt % and polyvinyl alcohol 6 wt %. The polymer is dried at 50-60 °C in vacuum oven before use. THF is 99 % pure and cannot be used without distillation. The assembly for the distillation of THF consists of three neck flask having collecting funnel and condenser attached to it at the top. THF is distilled at constant boiling point, anhydrous calcium oxide is added and solution is left overnight. After distillation, it was refluxed over sodium wire. The color of solution turned blue after the addition of benzophenone indicator, which after distillation is converted into colorless liquid and collected in collecting funnel placed above the three neck flask in assembly.

The polymer based nanocomposite thin films have been successfully prepared by utilizing prepared copper nanoparticles. Thin films of uniform thickness of compositions (5, 10, 15, 20, 25 wt % of synthesized nanoparticles) were prepared in poly (vinyl chloride-co-vinyl acetate-co- vinyl alcohol) by solution casting method.

A 5 wt % solution is prepared by dissolving 0.95 g of polymer in 20 mL THF by placing the solution on continuous magnetic stirring at room temperature. When the polymer is completely dissolved then adds 0.05 g of copper nanoparticles in above solution and kept the solution on stirring for 24 h. After stirring the solution was place in the ultrasonic bath for 30 mins at room temperature. The solution was poured in Teflon petri dish and placed on leveled surface at room temperature for 24 h to evaporate the solvent. Then uniform film was peeled off from the petri dish. The film was placed in vacuum oven for drying at 50-55 °C for 24 h. The general process of synthesis of films is as follows

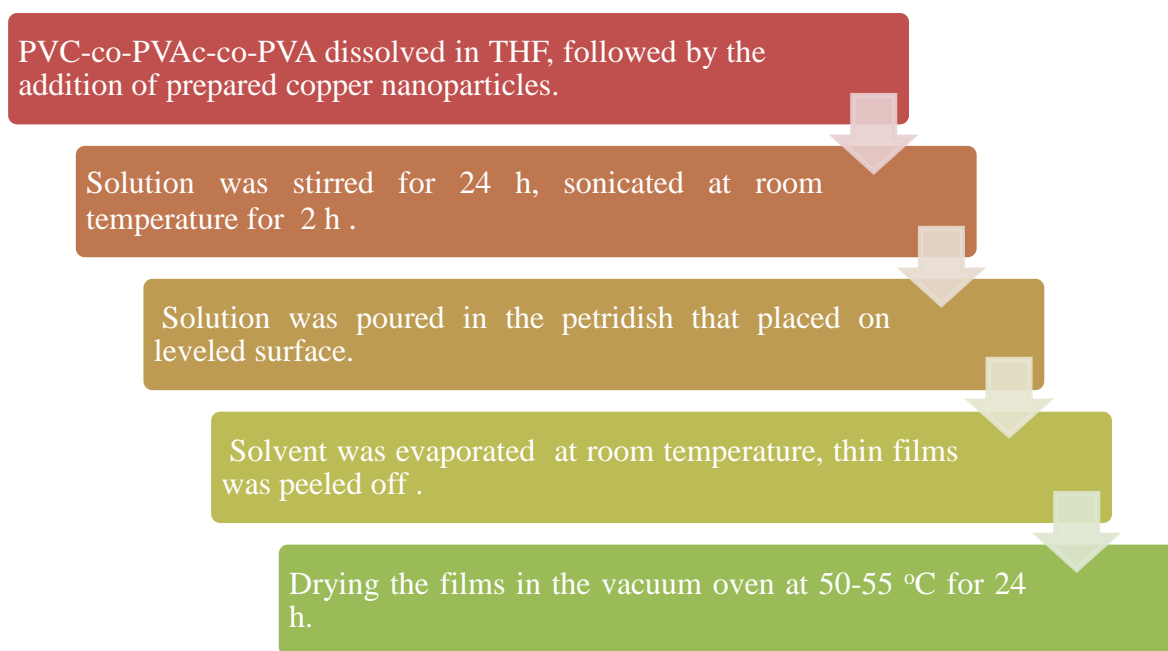


Figure 3.2: Flow sheet for the synthesis of films.

Similar procedure was employed to prepare the thin films of poly (vinyl chloride-co-vinyl acetate-co- vinyl alcohol)/Cu nanoparticles of four different compositions i.e. 10, 15, 20, and 25 wt %. Weight of polymer and nanoparticles required to synthesize films of different weight percentages are shown in Table 3.3.

Table 3.3: Weight percentages of PVC-co-PVAc-PVA and Copper nanoparticles used in the preparation of films.

S. No	Weight %	Weight of polymer (g)	Weight of CuNPs (g)	Volume of THF (mL)
1	0	1	0	20
2	5	0.95	0.05	20
3	10	0.90	0.1	20
4	15	0.85	0.15	20
5	20	0.80	0.2	20
6	25	0.75	0.25	20

Chapter 4

Results and Discussion

This chapter includes the structural, morphological and chemical characterization of prepared copper nanoparticles and thin films of copper nanocomposites along with their dielectric properties.

4.1 X-ray Powder Diffraction (XPRD)

Crystal structure, phase and crystallite size was measured by the X-ray diffraction technique. The XRD pattern of copper nanoparticles is shown in Fig 4.1. The crystals of copper nanoparticles are spherical in shape possessing cubic structure, space group Fm-3m (225) and the diffraction peaks are indexed to face centered cubic copper with lattice parameter $a=b=c=3.6150 \text{ \AA}$, $\alpha=\beta=\gamma=90^\circ$ showing characteristics diffraction peaks at $2\theta = 43.2^\circ$, 50.5° and 74.1° with corresponding planes at (111), (200), and (220) respectively. The crystallite size is found to be 33.5 nm. These results indicate the complete reduction of Cu^{+2} to Cu^0 . There is no peak corresponding to cupric oxide (CuO) at $2\theta=36^\circ$ indicates that pure copper nanoparticles without oxides are formed.

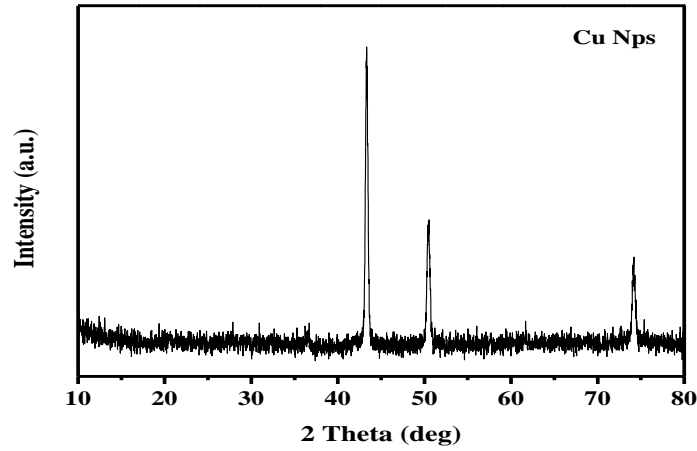


Figure 4.1: XPRD pattern of Copper nanoparticles.

The most quick and easy method to calculate the crystallite size is Debye-Scherrer's formula

$$D = \frac{K\lambda}{\beta \cos\theta}$$

Where

D=Crystallite size

K=Shape factor (0.94)

λ =Wavelength of Cu-K α (0.154 nm)

β =Full width half maxima (FWHM)

θ =Bragg's diffraction angle

The XRD of thin films containing 5, 10, 15, 20 and 25 wt % copper nanoparticles is shown in the Fig 4.2. The presence of broad peak or hump ranging from 10° to 30° centered at 22.7° corresponds to the polymer PVC-co-PVAc-co-PVA presenting the amorphous matrix of polymer. No crystallinity is produced in the polymer after the

addition of copper nanoparticles. The characteristics intense diffraction peak at $2\theta=43.2^\circ$, 50.5° and 74.1° that corresponds to Bragg's reflection of (111), (200), and (220) respectively are due to face centered cubic crystal of Cu^0 . The presence of extra peak at $2\theta=36.5$ corresponds to cupric oxide (CuO) reflects that some copper may oxidize during thin films casting due to intimate contact with atmospheric oxygen. The intensities of peak due to copper nanoparticles continue to increase with the increase in concentration of copper nanoparticles in thin films.

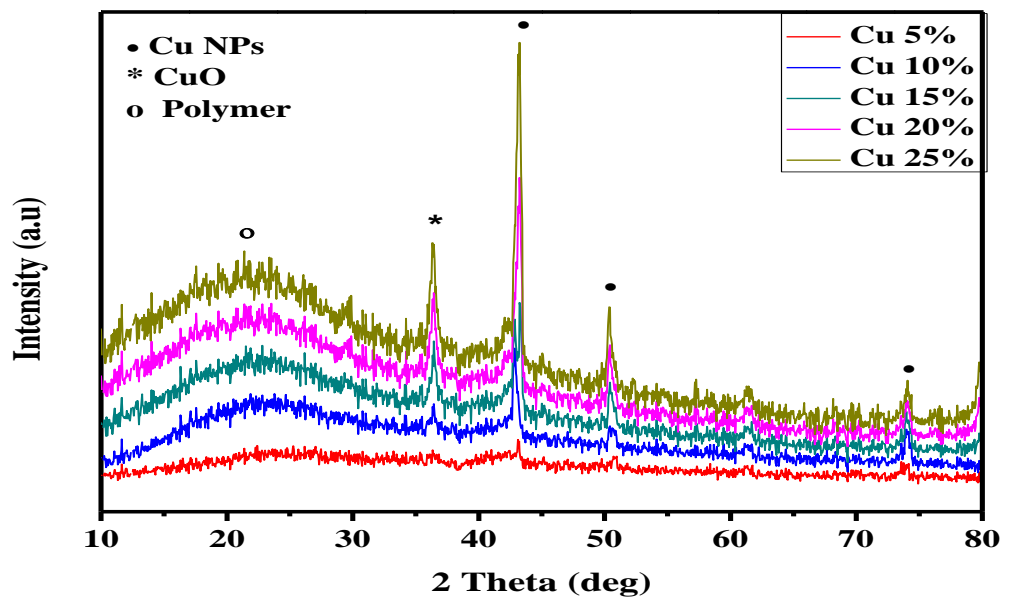


Figure 4.2: XPRD of PVC-co-PVAc-PVA/Copper nanocomposite films of various concentrations.

4.2 Field Emission Scanning Electron Microscopy (FESEM)

The surface topography and morphology of the samples were determined by SEM. The SEM micrographs and EDX spectra of copper nanoparticles is shown in Fig 4.3. The EDX spectra show that copper nanoparticles possess composition $\text{Cu}_{81.63} \text{O}_{16.44}$ and

Cl_{1.93} percent and particle size lies in the nano range. Copper nanoparticles are spherical in shape and well dispersed.

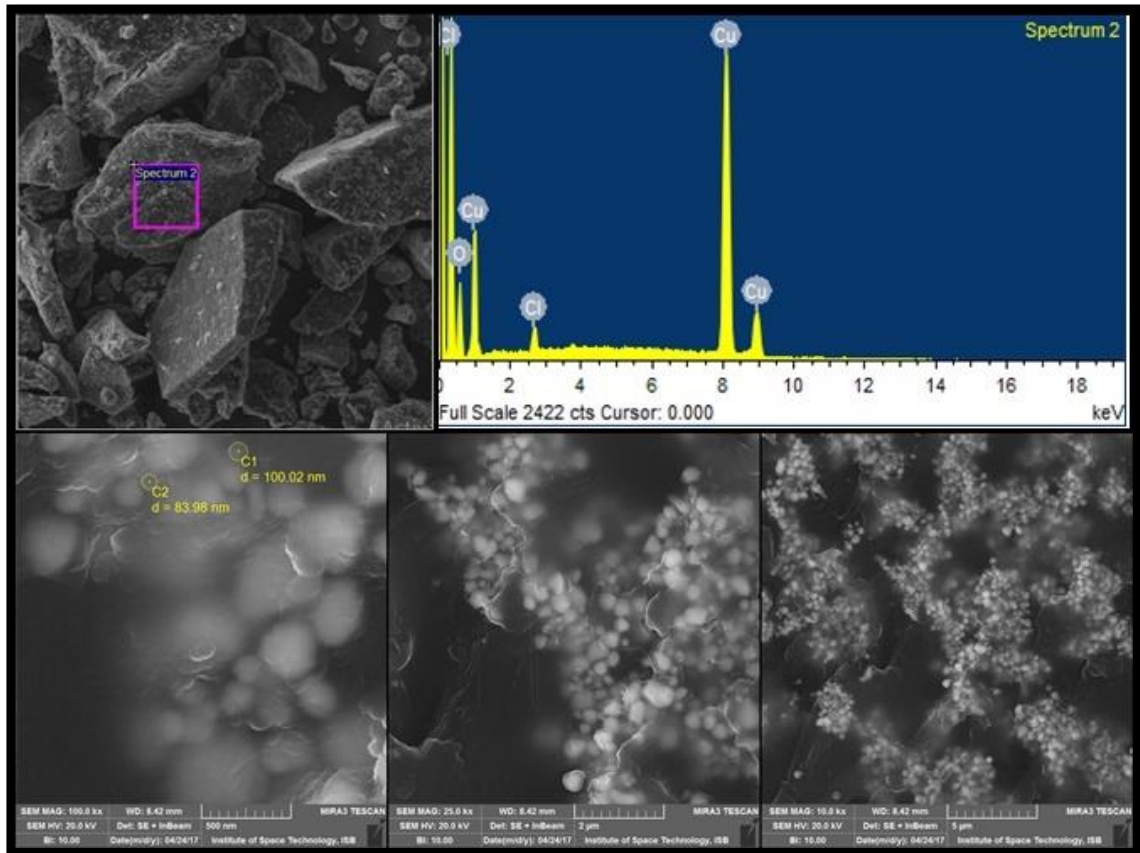


Figure 4.3: FESEM images and EDX spectra of Copper nanoparticles.

SEM investigates the size and dispersion of copper nanoparticles in composite films. The SEM micrographs showing nanoparticle particle distribution in thin films of different composition is shown in Fig 4.4(a-e). Copper nanoparticles are distributed in the polymer matrix but this distribution is not uniform. Ultrasonication helps to avoid agglomeration but still at some points particles agglomerates. In SEM micrograph 4.4a containing 5 % nanoparticles, particles clump at some points. While 10 % film shown in fig 4.4b particles are nonhomogenously distributed. In Fig 4.4c having 15 %

nanoparticles, also show agglomeration of particles but at few points. The particles are homogeneously distributed in films containing 20 and 25 % nanoparticles shown in Fig 4d and 4e respectively.

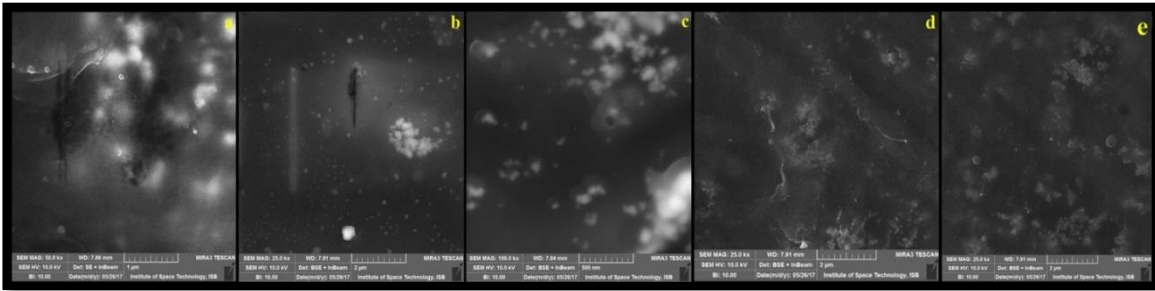


Figure 4.4(a-e): SEM micrographs of nanoparticles distribution in polymeric nanocomposite films.

The SEM micrographs showing particle size is shown in Fig 4.6(a-e). The average particle size of film containing 5, 10, 15, 20 and 25 wt % copper nanoparticles is 74.53, 57.93, 94.70, 72.63 and 47.53 nm respectively.

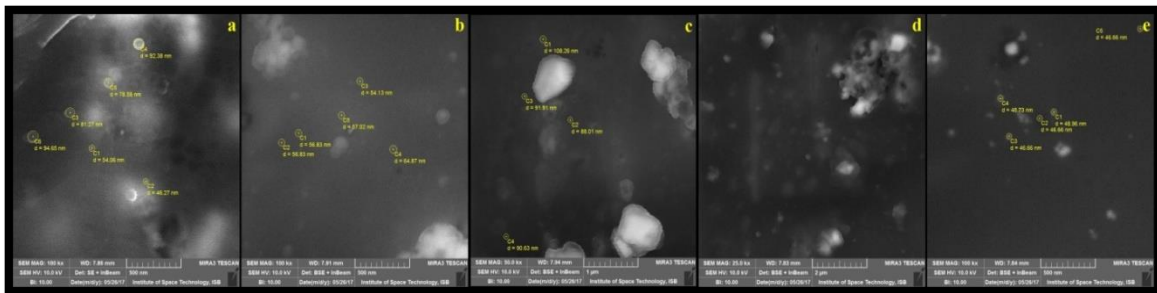


Figure 4.5(a-e): SEM micrographs showing particle size in polymeric nanocomposite films.

The EDX spectra of thin films containing 5, 10, 15, 20 and 25 wt % nanoparticles are shown in Fig 4.5(a-e). The EDX spectra indicate the composition of polymeric nanocomposite films having chlorine oxygen and copper nanoparticles. Carbon does not appear in spectra due to graphite coating whose peak is removed after analysis. The

composition of copper nanoparticles in EDX spectra corresponds to amount of copper nanoparticles actually added during synthesis of polymeric nanocomposite thin films.

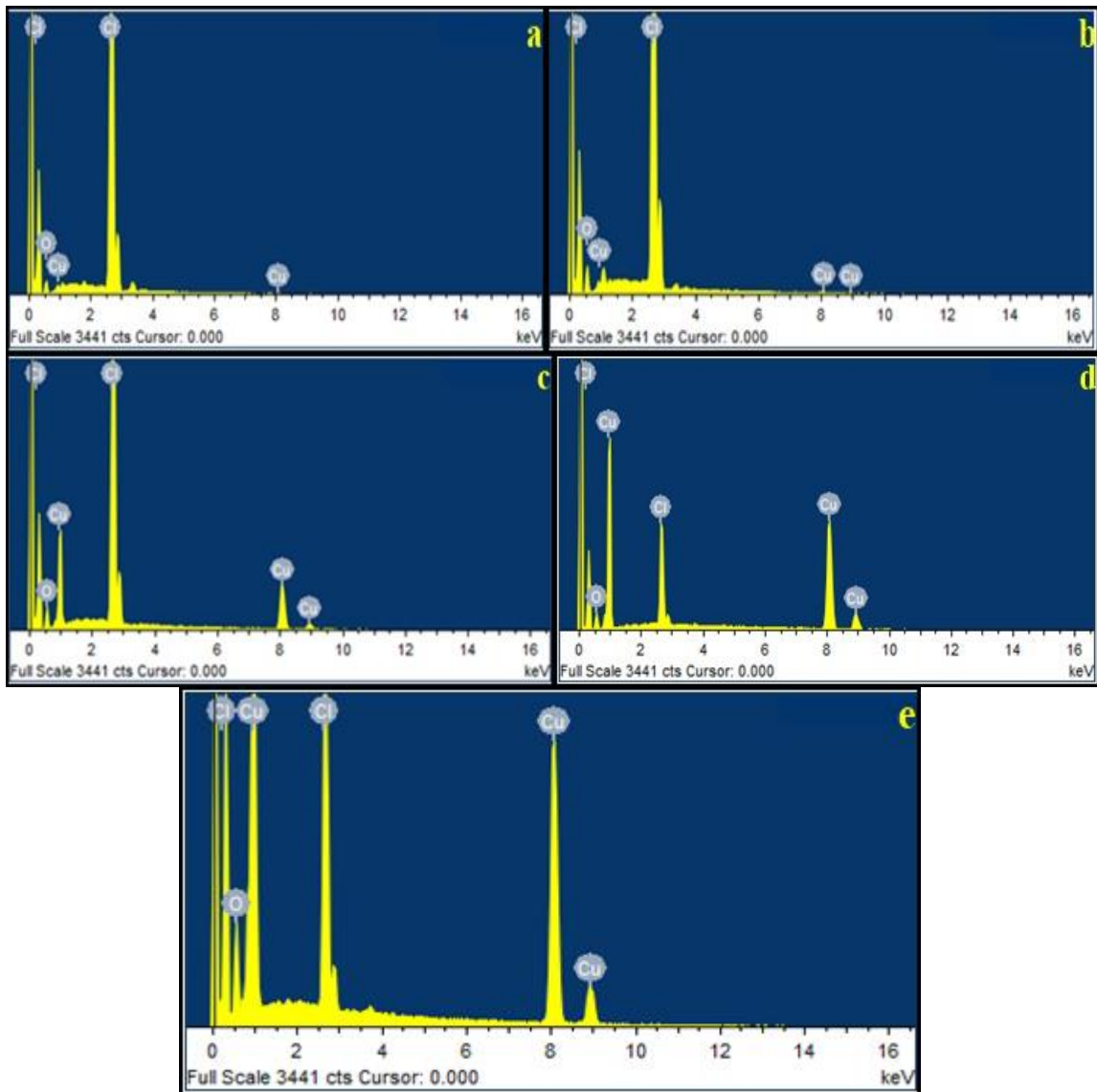


Figure 4.6(a-e) EDX spectra of nanocomposite films of various concentrations.

4.3 Fourier Transform Infrared Spectroscopy (FTIR)

FTIR analysis has been employed to analyze the vibrational bands of copper nanoparticles and poly (vinyl chloride-co-vinyl acetate-co- vinyl alcohol)/Copper nanocomposites. The IR spectrum of copper nanoparticles is shown in Fig 4.7. The IR band at 2990 cm^{-1} corresponds to C-H stretch in pyrrolidone ring. Sharp C=O stretching bands present in pyrrolidone is observed at 1645 cm^{-1} . Pyrrolidone ring stretch of medium and small intensity is observed at 1421 and 1367 cm^{-1} respectively. The band at 1271 cm^{-1} corresponds to C-N stretch in pyrrolidone ring. The bands at 1089 and 629 cm^{-1} is due to copper nanoparticles-poly (vinyl-pyrrolidone) hybrid [63].

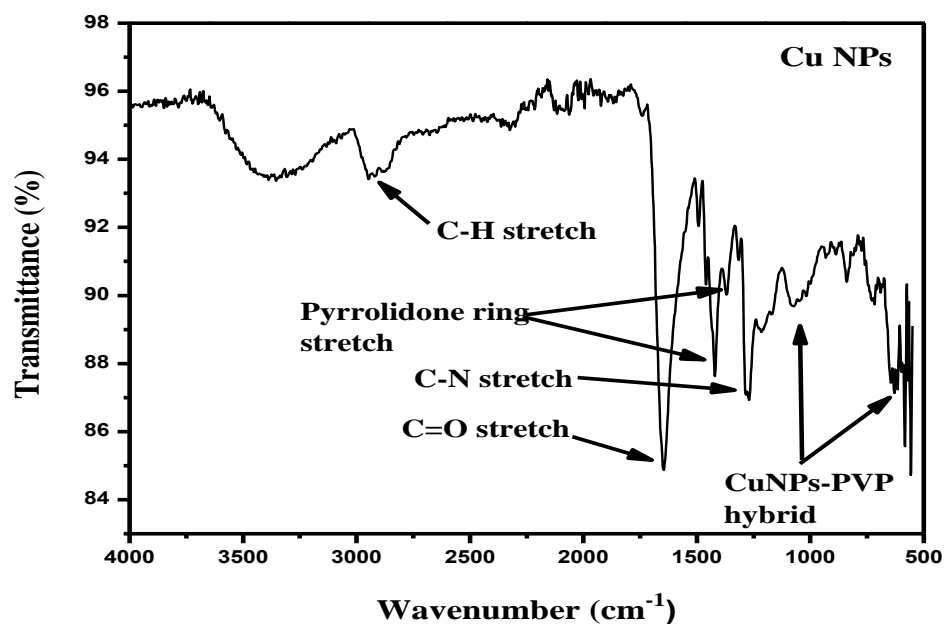


Figure 4.7: Infrared Spectra of Copper nanoparticles.

The IR spectra of thin films containing 5, 10, 15, 20 and 25 % copper nanoparticles are shown in the Fig 4.8. A broad O-H band centered at 3395 cm^{-1} corresponds to alcohol group in polymer. C-H stretch is observed at 2915 cm^{-1} . C=O group of acetate show

stretching band at 1740 cm^{-1} . C-O-C anti symmetric stretch is observed at 1250 cm^{-1} while C-Cl stretch is seen at 615 cm^{-1} . C=O group in pyrrolidone ring show stretch at 1655 cm^{-1} . Pyrrolidone ring stretch is observed at 1427 cm^{-1} . The C-N stretch of pyrrolidone ring is overlapped with C-O-C stretch of acetate at 1250 cm^{-1} with slight increase in band intensity. The hybrid of copper nanoparticles-poly (vinyl-pyrrolidone) shows two stretching bands at 1089 and 675 cm^{-1} [63]. IR spectrum of polymeric nanocomposite of different concentrations shows individual bands for copper nanoparticle and poly (vinyl chloride-co-vinyl acetate-co- vinyl alcohol) that shows that no chemical interactions take place during the synthesis of polymeric nanocomposites. The intensity of bands decreases successively with increase in weight % of nanoparticles.

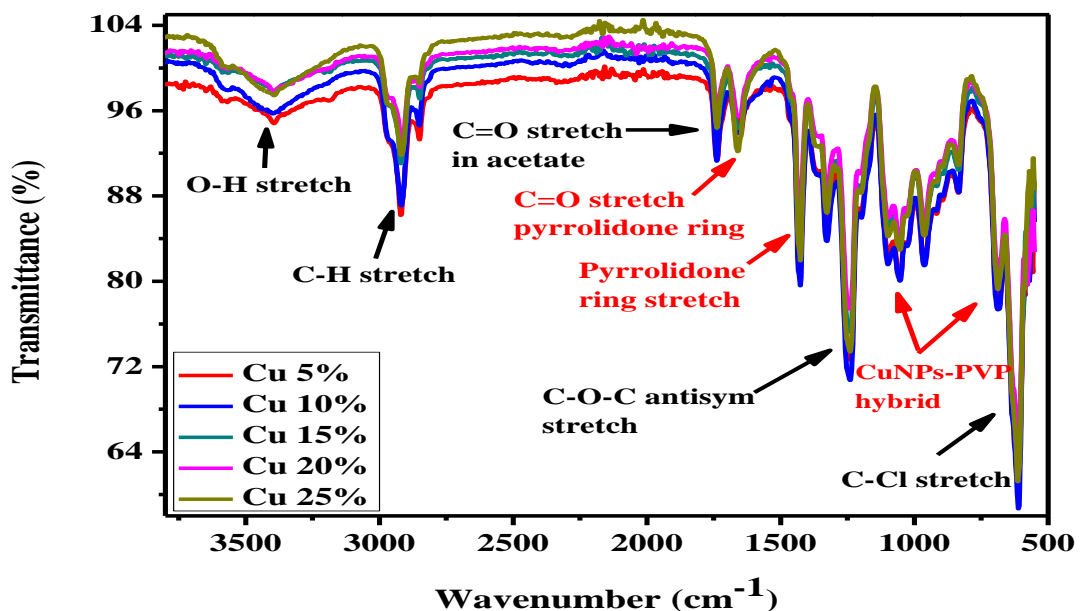


Figure 4.8: IR spectra of Copper nanocomposite films of various concentrations.

4.4 Properties

4.4.1 Dielectric Properties:

Dielectrics are the material having electrical dipoles permanently. They are insulators having no effect of applied electrical field and hence are used to store electrical energy. Four important parameters of dielectric properties are dielectric constant, dielectric loss, tangent loss and AC conductivity. Dielectric constant is the ratio of permittivity of a substance to the permittivity of free space. Dielectric constant (ϵ) is calculated by the expression given below [71].

$$\epsilon = \frac{C \times d}{\epsilon_0 \times A}$$

Where

C= Capacitance

d= Thickness of sample

ϵ_0 = Permittivity of free space having value $8.85 \times 10^{-12} \text{ Fm}^{-1}$

A= Area of sample

Dielectric loss quantifies a dielectric material's inherent dissipation of electromagnetic energy due to the alignment of particles along the applied field. Dielectric loss (ϵ'') is the imaginary part for the determination of electromagnetic energy. Dielectric loss is calculated by formula [71].

$$\epsilon'' = \epsilon \times \text{Dissipation factor}$$

The real part to calculate the energy loss is tangent loss (δ) calculated by the formula [71].

$$\tan \delta = \epsilon'' / \epsilon$$

AC conductivity (σ_{AC}) is ability of material to pass electric current and can be calculated by the formula [72].

$$\sigma_{AC} = 2\pi f \epsilon_0 \epsilon'' \tan \delta$$

Figure 4.9 indicates the frequency dependent behavior of dielectric constant of prepared films of different compositions and unfilled polymer matrix. It can be seen that in 5 % and 10 % filler loading the dielectric constants are lower than unfilled polymer at all frequencies. This reduction in dielectric constant is either because of entanglement of polymeric chains due to the dispersion of nanoparticles in polymer matrix or dispersion of nanoparticles in polymer matrix causes the formation of thin immobile polymer nanolayers around nanoparticles surface due to strong bonding of nanoparticles with polymer [73]. These two interaction dynamics operate simultaneously and it is difficult to understand properly and need further studies. With the increase in filler loading interfacial polarization increase that causes increase in the value of dielectric constants for films having 15 %, 20 % and 25 % of copper nanoparticles. The dielectric constant for film having 25 % copper loading reaches at its maximum value of 3.75 which then decrease linearly with value of 3.25 and 3.12 for 20 % and 15 % loadings respectively.

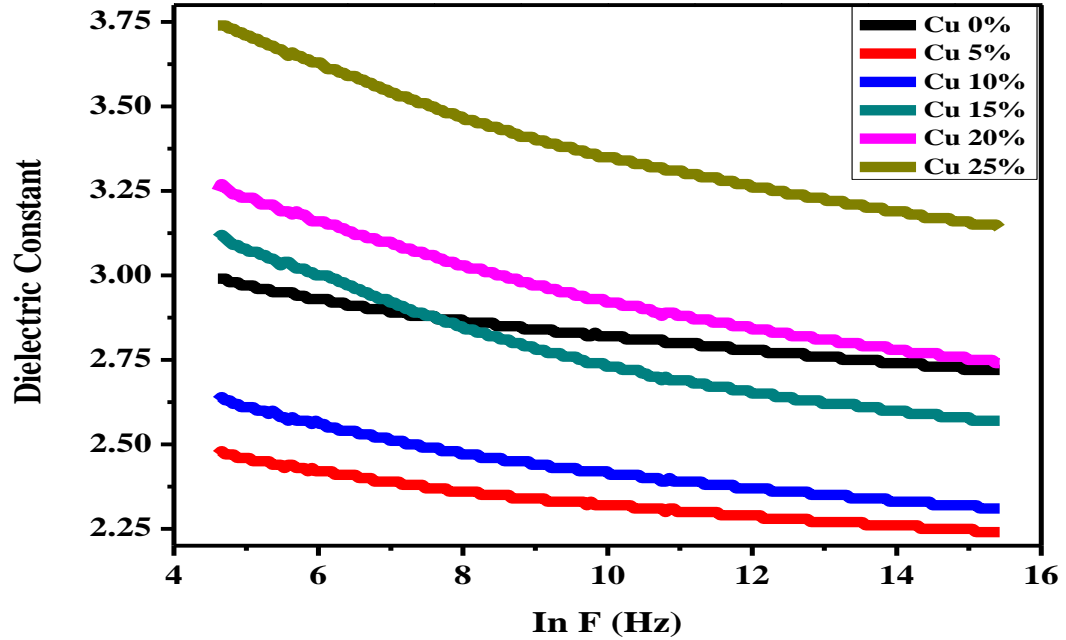


Figure 4.9: Dielectric constant of Copper nanocomposite films of various concentrations.

Dielectric loss as a function of frequency and filler loading is shown in Fig 4.10. The dielectric loss increases with the increase in the filler loading. Lowest dielectric loss is seen for the film having 5 % copper nanoparticles which then continues to increase up to the maximum value of 0.16 for the films containing 20 % and 25 % copper loadings both films possess comparable dielectric loss. This continual increase in dielectric loss is consistent with above mentioned reason of interfacial polarization that is effectively operating in nanocomposite films as well as interfacial interaction between copper nanoparticles and polymer matrix [70].

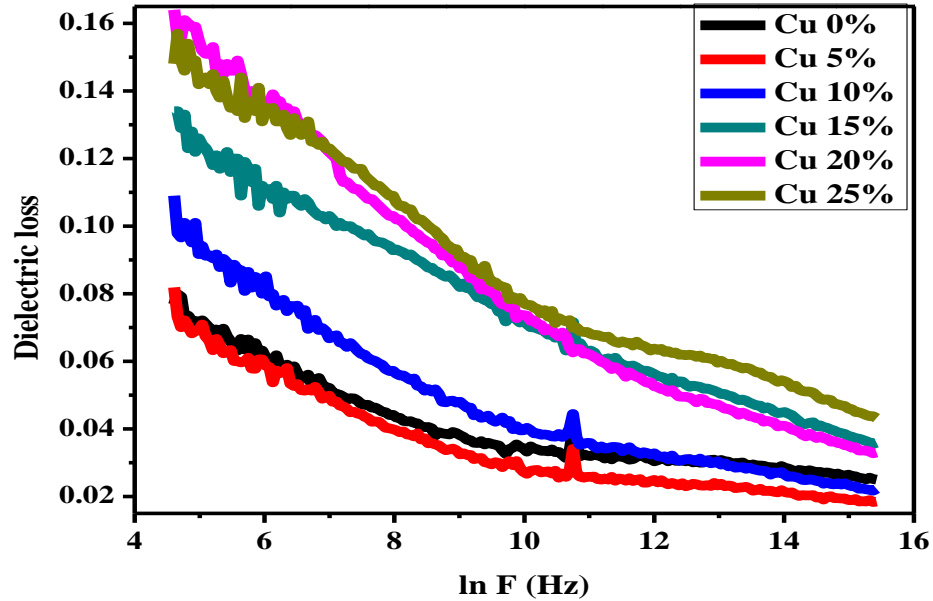


Figure 4.10: Dielectric loss of Copper nanocomposite films of various concentrations.

The variation of tan delta with respect to frequency is shown in Fig 4.11. Tan delta depends on conductivity which is related to the number of charge carriers in composite films. Dielectric materials having less dissipation factor shows better performance for the charge storage application and can be used in super capacitors. High dielectric constant combined with low dielectric loss leads to reduced dissipation factor and enhanced dielectric properties.

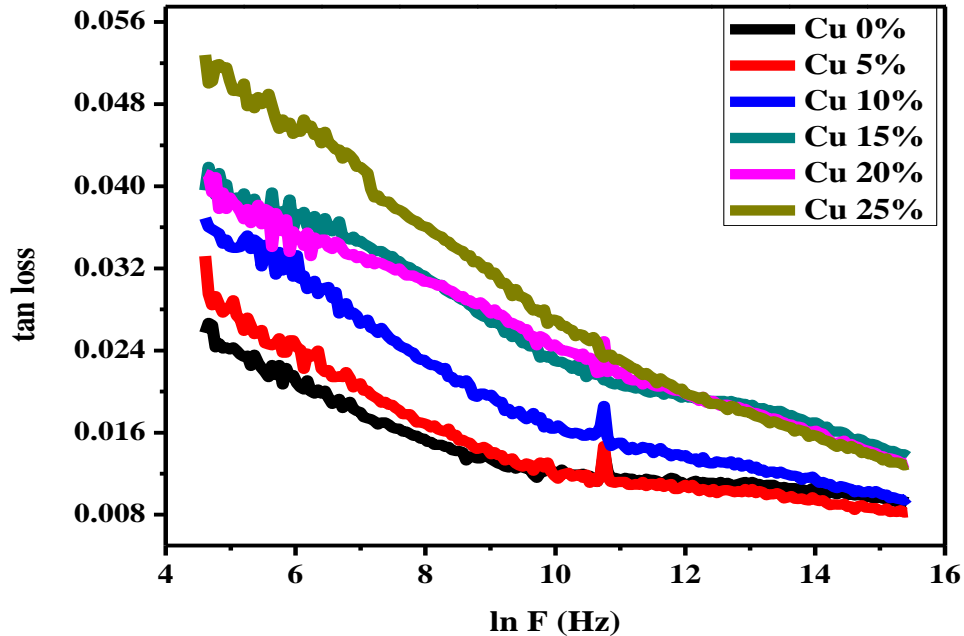


Figure 4.11: Tan loss of Copper nanocomposite films of various concentrations.

AC conductivity of composite film increases with increase in copper loading. Maximum conductivity of value 1.2×10^{-5} S/m is recorded for sample containing 25 % copper nanoparticles. This gradual increase in the conductivity is due to larger dielectric dispersion originating from development of interfacial polarization. There is no drastic increase in conductivity with increase in filler loading. This shows that there is no proper conductive pathway formed because of presence of small amount of cuprous oxide along with copper nanoparticle. Presence of small amount of cuprous oxide along with copper nanoparticles in films prevents the direct contact between copper nanoparticles thus averting the formation of well-established conducting network. Secondly percolation threshold is reached when filler loading is increased but increased loading up to certain extent by *ex-situ* method would leads to agglomeration. Therefore electric dispersion plays an important role in contributing to AC conductivity at higher frequencies [11, 70].

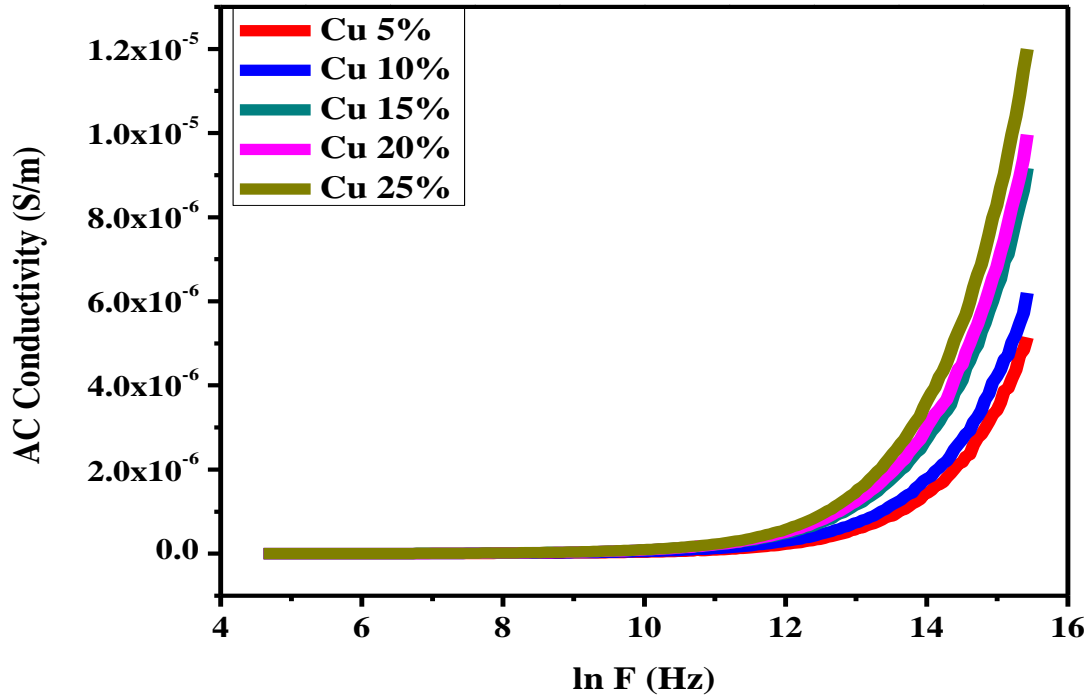


Figure 4.12: AC conductivity of Copper nanocomposite films of various concentrations.

4.5 Conclusion and Future Prospects:

Copper nanoparticles have been successfully prepared by environmentally friendly method and polymeric nanocomposite films of various concentrations by solution casting method. The composition, morphology, particle size and crystallite size has been investigated by SEM, XRD and FTIR analysis. Dielectric properties are measured which shows that polymeric nanocomposite films possess higher dielectric constant as compared to the polymer and very low dielectric loss of 0.08 has been reported which makes such type of nanocomposite films a better material to be used in electronic circuit and super capacitors. Adding ceramics along with the copper nanoparticles in the films would result in further increase in value of dielectric constant and lowers the dielectric loss

and this enhancement in properties would lead to use of these types of polymeric nanocomposite films in sensitive electronic circuits.

References

- [1] Gribbin, John and M. Gribbin, "Richard Feynman: A Life in Science. Dutton," **17**, (1997).
- [2] Gleiter H, "Materials with ultrafine microstructures: retrospectives and perspectives," *Nanostructured Materials.*, **1**, pp. 1-19, (1992).
- [3] R. M. Wang, S. R. Zheng and Y. P. Zheng, "Introduction to polymer matrix composite," *Polymer Matrix Composites and Technology.*, **547-548**, pp. 1-25, (2011).
- [4] P. H. C. Camargo, K. G. Satyanarayana and F. Wypych, "Nanocomposites: synthesis, structure, properties and new application opportunities," *Material Research.*, **12**, (2006).
- [5] K. Akamatsu, S. Ikeda, H. Nawafune and S. Deki, "Surface Modification-Based Synthesis and Microstructural Tuning of Nanocomposite Layers: Monodispersed Copper Nanoparticles in Polyimide Resins," *Chem Material.*, **15**, pp. 2488–2491, (2003).
- [6] M. Tyagi and D. Tyagi, "Polymer Nanocomposites and their Applications in Electronics Industry," *Int. J. Electron. Electr. Engineering.*, **7**, pp. 603-608, (2014).
- [7] D.K. Avasthi, Y.K. Mishra, D. Kabiraj and N.P Lalla, "Synthesis of metal-polymer nanocomposites for optical applications," *J. Nanotechnol.*, **18**, pp. 125604, (2007).
- [8] A. Leszczynska, J. Njuguna, K. Pielichowski and J.R. Banerjee, "Polymer/montmorillonite nanocomposites with improved thermal properties," *Thermochimica acta.*, **453**, pp. 75-96, (2007).
- [9] J. W. Gilman, T. Kashiwagi, A. B. Morgan, R. H. Harris Jr, L. Brassell, W. H. Awad, R. D. Davis, L. Chyal, T. Sutto, P. C. Trulove and H. DeLong, "Recent Advances in Flame Retardant Polymer Nanocomposites,"
- [10] A. Choudhury, "Polyaniline/silver nanocomposites: Dielectric properties and ethanol vapour sensitivity," *Sens. Actuator B-Chem.*, **138**, pp. 318–325 (2009).
- [11] A. B. da Silva, M. Arjmand , U. Sundararaj and R. E. S. Bretas, "Novel composites of copper nanowire/PVDF with superior dielectric properties," *Polymer.*, **55**, pp. 226-234, (2014).
- [12] Y. Rao, S. Ogitani, P. Kohl and C. P. Wong, "Novel polymer–ceramic nanocomposite based on high dielectric constant epoxy formula for embedded capacitor application," *J. Appl. Polym. Sci.*, **83**, pp. 1084-1090, (2001).
- [13] S. Singha and M. J. Thomas, "Dielectric Properties of Epoxy Nanocomposites,"

- IEEE Transactions on Dielectrics and Electrical Insulation.*, **15**, pp. 12-23, (2008).
- [14] Y. Kojima, A. Usuki, M. Kawasumi, A. Okada, T. Kurauchi and O. Kamigaito, "Synthesis of Nylon 6-Clay Hybrid by Montmorillonite Intercalated with ϵ Caprolactam," *J. Polym Sci.A.*, **31**, pp. 983-986, (1993).
- [15] J. Wang, X. Wang, C. Xu, M. Zhang and X. Shang, "Preparation of graphene/poly(vinyl alcohol) nanocomposites with enhanced mechanical properties and water resistance," *polym Int.*, **60**, pp. 816-822, (2011).
- [16] X. Huang, P. Jiang, and L. Xie, "Ferroelectric polymer/silver nanocomposites with high dielectric constant and high thermal conductivity," *App. Phys. Lett.*, **95**, pp. 242901-3, (2009).
- [17] M. Baibar, and P. G. Romero, "Nanocomposites based on conducting polymers and carbon nanotubes: from fancy materials to functional applications," *J Nanosci Nanotechnol.*, **6**, pp. 289-302, (2006).
- [18] I. Dinca, C. Ban, A. Stefan and G. Pelin, "Nanocomposites as Advanced Materials for Aerospace Industry," *INCAS BULLETIN.*, **4**, pp. 73-83, (2012).
- [19] A. K. Gaharwar, N. A. Peppas and A. Khademhossein, "Nanocomposite hydrogels for biomedical applications," *Biotechnol Bioeng.*, **111**, pp. 441-453, (2013).
- [20] Z. Liu, J. T. Robinson, X. Sun, and H. Dai, "PEGylated Nanographene Oxide for Delivery of Water-Insoluble Cancer Drugs," *J. Am. Chem. Soc.*, **130**, pp. 10876-10877, (2008).
- [21] E. R. Gillies and J. M. J. Frechet, "Dendrimers and dendritic polymers in drug delivery," *Drug Discovery Today.*, **10**, pp. 35-43, (2005).
- [22] S. Shankar and J. W. Rhim, "Polymer Nanocomposites for Food Packaging Applications," *Functional and Physical Properties of Polymeric Nanocomposites.*, pp 29-55 (2016).
- [23] M. Avella, J. J. D. Vlieger, M. E. Errico, S. Fischer, P. Vacca and M. G. Volpe "Biodegradable starch/clay nanocomposite films for food packaging applications," *Food chem.*, **93**, pp. 467-474, (2005).
- [24] X. Song, S. Sun, W. Zhang and Z. Yin, "A method for the synthesis of spherical copper nanoparticles in the organic phase," *J. Colloid Interface Sci.*, **273**, pp. 463-469, (2004).
- [25] M. A. Al-Mamun, Y. Kusumoto and M. Muruganandham, "Simple new synthesis of copper nanoparticles in water/acetonitrile mixed solvent and their characterization," *Mater. Lett.*, **63**, pp. 2007-2009, (2009).
- [26] Y. Kobayashi, S. Ishida, K. Ihara, Y. Yasuda, T. Morita and S. Yamada, "Synthesis of metallic copper nanoparticles coated with polypyrrole," *Colloid. Polym. Sci.*, **287**, pp. 877-880, (2009).
- [27] G. Granata, T. Yamaoka, F. Pagnanelli and Akio Fuwa, "Study of the synthesis of

- copper nanoparticles: the role of capping and kinetic towards control of particle size and stability,” *J. Nanopart. Res.*, **18**, pp. 1-12, (2016).
- [28] T. M. D. Dang, T. T. T. Le, E. F. Blanc and M. C. Dang, “Synthesis and optical properties of copper nanoparticles prepared by a chemical reduction method,” *Adv. Nat. Sci.: Nanosci. Nanotechnol.*, **2**, pp. 015009-015015, (2001).
- [29] Q. I. Zhang, Z. M. Yang, B. J. Ding, X. Z. Lan and Y. J. Guo, “Preparation of copper nanoparticles by chemical reduction method using potassium borohydride” *Trans. Nonferrous Met. Soc. China.*, **20**, pp. 240-244, (2010).
- [30] N. A. Dhas, C. P. Raj and A. Gedanken, “Synthesis, Characterization, and properties of metallic copper nanoparticles,” *Chem. Mater.*, **10**, pp. 1446-1452, (1998).
- [31] S. S. Jushi, S.F. Pat, V. Iyer and S. Mahumuni, “Radiation induced synthesis and characterization of copper nanoparticles,” *Nanostructure Mater.*, **10**, pp. 1135-1144, (1998).
- [32] R.M. Tilaki, A. I. Zad and S.M. Mahdavi, “Size, composition and optical properties of copper nanoparticles prepared by laser ablation in liquids” *Appl. Phys. A.*, **88**, pp. 415–419 (2007).
- [33] Ti Nakamura, Y. Tsukahara, T. Sakata, H. Mori, Y. Kanbe, H. Bessho and Y. Wad, “Preparation of Monodispersed Cu Nanoparticles by Microwave-Assisted Alcohol Reduction,” *Chem. Soc. Jpn.*, **80**, pp. 224–232, (2007).
- [34] M. Blosi, S. Albonetti, M. Dondi, C. Martelli and G. Baldi, “Microwave-assisted polyol synthesis of Cu nanoparticles,” *J. Nanopart. Res.*, **13**, pp. 127–138 (2011).
- [35] J. S. Cerda, H. E. Gomez, G. A. Nunez, I. A. Rivero, Y. G. Ponce, L. Z. F. Lopez, “A green synthesis of copper nanoparticles using native cyclodextrins as stabilizing agents,” *Journal of Saudi Chemical Society.*, **21**, pp. 341-348, (2016).
- [36] V. D. Kulkarni and P. S. Kulkarni, “Green synthesis of copper nanoparticles using osmium sanctum leaf extract,” *Int. J. Chem. Stud.*, **1**, pp. 1-4, (2013).
- [37] J. P. Cason and C. B. Roberts, “Metallic copper nanoparticle synthesis in AOT reverse micelles in compressed propane and supercritical ethane solutions,” *J. Phys. Chem. B.*, **104**, pp. 1217-1221, (2000).
- [38] S. I. Cha, C. B. Mo, K. T. Kim, Y. J. Jeong and S. H. Honga, “Mechanism for controlling the shape of Cu nanocrystals prepared by the polyol process.” *J. Mater. Res.*, **21**, pp. 2371-2378, (2006).
- [39] M. Hosseini, D. H. Fatmehsari and S.P. H. Marashi, “Synthesis of different copper nanostructures by the use of polyol technique” *Appl. Phy. A.*, **120**, pp. 1579-1586, (2015).
- [40] B. K. Park , S. Jeong , D. Kim , J. Moon , S. Lim , J. S. Kim, “Synthesis and size control of monodisperse copper nanoparticles by polyol method,” *J. Colloid Interface Sci.*, **311**, pp. 417–424, (2007).
- [42] I. Lisiecki and M. P. Pileni, “Synthesis of Copper Metallic Clusters Using

- Reverse Micelles as Microreactors,” *J. Am. Chem. Soc.*, **115**, pp. 3887-3896, (1993).
- [42] F. Fievet, F. F. Vincent, J. P. Lagier, B. Dumont and M. Figlarzb, “Controlled nucleation and growth of micrometer size copper particles prepared by the polyol process,” *J. MATER. CHEM.*, **3**, pp. 627-632, (1993).
- [43] H. T. Zhu, C. Y. Zhang and Y. S. Yin, “Rapid synthesis of copper nanoparticles by sodium hypophosphite reduction in ethylene glycol under microwave irradiation,” *J. Cryst Growth.*, **270**, pp. 722–728, (2004).
- [44] S. I. Cha, C. B. Mo, K. T. Kim, Y. J. Jeong, and S. H. Hong, “Mechanism for controlling the shape of Cu nanocrystals prepared by the polyol process,” *J. Mater. Res.*, **21**, pp. 2371-2378, (2006).
- [45] T. G. Altincekic and I. Boz, “Influence of synthesis conditions on particle morphology of Nanosized Cu/ZnO powder by polyol method,” *Bull. Mater. Sci.*, **31**, pp. 619–624, (2008).
- [46] K. J. Carroll, J. U. Reveles, M. D. Shultz, S. N. Khanna and E. E. Carpenter, “Preparation of Elemental Cu and Ni Nanoparticles by the Polyol Method: An Experimental and Theoretical Approach,” *J. Phy. Chem.*, **115**, pp. 2656-2664, (2011).
- [47] A. Sarkar, T. Mukherjee, and S. Kapoor, “PVP-Stabilized Copper Nanoparticles: A Reusable Catalyst for “Click” Reaction between Terminal Alkynes and Azides in Nonaqueous Solvents,” *J. Phys. Chem.*, **112**, pp. 3334-3340, (2008).
- [48] A. M. R. Gallettia, C. Antonettia, M. Marraccib, F. Piccinellia, Bernardo Tellini, “Novel microwave-synthesis of Cu nanoparticles in the absence of any stabilizing agent and their antibacterial and antistatic applications,” *Appl. Surf. Sci.*, **280**, pp. 610-618, (2013).
- [49] M. N. K. Chowdhury, M. D. H. Beg, M. R. Khan, M. F. Mina “Synthesis of copper nanoparticles and their antimicrobial performances in natural fibres” *Mater. Lett.*, **88**, pp. 26-29, (2013).
- [50] E. S. Aazam and W. A. El-Said, “Synthesis of Copper/Nickel Nanoparticles using Newly Synthesized Schiff-base Metals Complexes and their Cytotoxicity/Catalytic Activities,” *bio. Organic. chem.*, **57**, pp. 5-12, (2014)
- [51] S. Kubotaa, T. Moriokaa, M. Takesueb, H. Hayashic, M. Watanabeb and R. L. Smith Jr., “Continuous supercritical hydrothermal synthesis of dispersible zero-valent copper nanoparticles for ink applications in printed electronic,” *J. Supercrit. Fluids.*, **86**, pp. 33-40, (2013).
- [52] J. S. Kang, H. S. Kim, J. Ryu, H. T. Hahn, S. Jang and J. W. Joung “Inkjet printer electronics using copper nanoparticle ink,” *J. Mater. Sci.*, **21**, pp. 1213-1220, (2010).
- [53] S. Magdassi, M. Grouchko and A. Kamyshny, “Copper Nanoparticles for Printed Electronics: Routes Towards Achieving Oxidation Stability,”

- Materials.*, **3**, pp. 4626-4638 (2010).
- [54] G. Y. Yurkov, A. V. Kozinkin, T. I. Nedoseikina, A. T. Shuvaev, V. G. Vlasenk, S. P. Gubin, and I. D. Kosobudskii, "Copper Nanoparticles in a Polyethylene Matrix," *Inorganic Material.*, **37**, pp. 997–1001, (2001).
- [55] S. Ikeda, K. Akamatsu, H. Nawafune, T. Nishino and S. Deki, "Formation and Growth of Copper Nanoparticles from Ion-Doped Precursor Polyimide Layers," *J. Phys. Chem. B.*, **108**, pp. 15599-15607, (2004).
- [56] N. Cioffi, N. Ditaranto, L. Torsi, R. A. Picca, E. De Giglio, L. Sabbatini, L. Novello, G. Tantillo, T. Bleve-Zacheo and P. G. Zambonin, "Synthesis, analytical characterization and bioactivity of Ag and Cu nanoparticles embedded in polyvinyl-methyl-ketone films," *Anal. Bioanal. Chem.*, **382**, pp. 1912–1918, (2005).
- [57] H. Palza, S. Gutierrez, K. Delgado, O. Salazar, V. Fuenzalida, J. I. Avila, G. Figueroa and R. Quijada, "Toward Tailor-Made Biocide Materials Based on Poly(propylene)/Copper Nanoparticles," *Macromol. Rapid. Commun.*, **31**, pp. 563–567 (2010).
- [58] I. R. Kamrupi and S. K. Dolui, "Synthesis of Copper–Polystyrene Nanocomposite Particles Using Water in Supercritical Carbon Dioxide Medium and Its Antimicrobial Activity," *J. Appl. Polym. Sci.*, **120**, pp. 1027–1033, (2011).
- [59] K. Tian, C. Liu, H. Yang and X. Ren, "In situ synthesis of copper nanoparticles/polystyrene composite," *Colloids. Surf. A: Physicochem. Eng. Asp.*, **397**, pp. 12– 15, (2012).
- [60] T. Xu, C. Li, H. Li, J. Bai, H. Qin and W. Sun, "Synthesis of well-dispersed copper nanoparticles in electrospun polyacrylonitrile Nanofibers," *Micro. Nano. Lett.*, **8**, pp. 849–852, (2013).
- [61] A. Guzman, J. Arroyoa, L. Verdea and J. Rengifo, "Synthesis and characterization of copper nanoparticles/polyvinylchloride (Cu NPs/PVC) nanocomposites," *Procedia Mater., Sci.*, **9**, pp. 298 – 304, (2015).
- [62] M. Safiullah, A. WasiK and A. Bashak, "Preparation of poly(Glycidyl methacrylate)–copper nanocomposite by in-situ suspension polymerization – A novel synthetic method," *Mater. Lett.*, **133**, pp. 60–63, (2014).
- [63] M. Bambo, R. Moutloali and R. Krause, "Polymer Nanocomposite of PVDF/Organoclay-Copper Nanoparticles hybrid: Synthesis and Characterization," *Mater. Today.*, **2**, pp. 3921 – 3931(2015).
- [64] A. Nithyaa, S. C. Mohana, K. I. Jeganathanb and K. Jothivenkatachalam, "A potential photocatalytic, antimicrobial and anticancer activity of chitosan-copper nanocomposite," *Int. J. Bio, Macromolec.*, **104**, pp. 1774-1782, (2017).
- [65] U. Nadeem, Z. Ahmad, S. Zulfiqar and M. I. Sarwar, "Co-poly(vinyl chloride-vinyl acetate-vinyl alcohol)-Silica Nanocomposites from Sol–Gel Process: Morphological, Mechanical, and Thermal Investigations, " *J. Appl. Polym.*, (2012).

- [66] M. Benounis, “Novel phosphate-selective poly(vinyl chloride-co-vinylacetate-co-vinyl alcohol) membrane optode with carrier based on tin compound” *Sens. Actuators. B. Chem.*, **216**, pp. 57–63, (2015).
- [67] F. Karimi and B. A. Peppley, “Comparison of conventional versus microwave heating for polyol synthesis of supported iridium based electrocatalyst for polymer electrolyte membrane water electrolysis,” *Intl. J. Hydrog. Energy.*, **42**, pp. 5083-5094, (2017).
- [68] T. Zhao, R. Sun, S. Yu, Z. Zhang, L. Zhou, H. Haung and R. Du, “Size-controlled preparation of silver nanoparticles by a modified polyol method,” *Colloids Surf A Physicochem Eng Asp.*, **366**, pp. 197-202, (2010).
- [69] F. Fievet, J.P. Lagier, B. Blin, B. Beaudoin and M.Figlarz, “Homogeneous and heterogeneous nucleations in the polyol process for the preparation of micron and submicron size metal particles,” *Solid state ionics.*, **32-33**, pp. 198-205, (1989).
- [70] G. Li, S. Yu , R. Sun and D. Lu, “Clean and in-situ synthesis of copper–epoxy nanocomposite as a matrix for dielectric composites with improved dielectric performance,” *COMPOS. SCI. TECHNOL.*, **110**, pp. 95–102, (2015).
- [71] I. H. Gul and A. Maqsood, “Structural, magnetic and electrical properties of cobalt ferrites prepared by the sol-gel route,” *J. Alloys Compd.*, **465**, pp. 227–231, (2008).
- [72] J. K. Rao, A. Raizada, D. Ganguly, M. M. Mankad, S. V. Satyanarayana, and G. M. Madhu, “Investigation of structural and electrical properties of novel CuO-PVA nanocomposite films,” *J. Mater. Sci.*, **50**, pp. 7064–7074, (2015).
- [73] S. Singha and M. Joy Thomas, “Dielectric Properties of Epoxy Nanocomposites” *IEEE Transactions on Dielectrics and Electrical Insulation*, **15**, (2008).